Technische Universität Kaiserslautern
Fachbereich Chemie

Characterization of Electronically Excited States of Reactive Molecules by Combined IR/UV Spectroscopy

Am Fachbereich Chemie der Technischen Universität Kaiserslautern zur Erlangung des akademischen Grades „Doktor der Naturwissenschaften“ eingereichte

Dissertation

vorgelegt von
Dipl.-Chem. Kristina Bartl

Betreuer: Prof. Dr. Markus Gerhards

Tag der wissenschaftlichen Aussprache: 18.06.2009

Die vorliegende Arbeit wurde in der Zeit von August 2006 bis Mai 2009 angefertigt: In der Zeit von August 2006 bis April 2008 wurde die Arbeit am Institut für Physikalische Chemie I der Heinrich-Heine-Universität Düsseldorf erstellt, fortgesetzt und beendet wurde die Arbeit in der Zeit von April 2008 bis Mai 2009 an der Technischen Universität Kaiserslautern.

Datum des Antrags auf Eröffnung des Promotionsverfahrens: 19.11.2008
Tag der wissenschaftlichen Aussprache: 18.06.2009

Promotionskomission:
Vorsitzender: Prof. Dr. J. Hartung
1. Berichterstatter: Prof. Dr. M. Gerhards
2. Berichterstatter: Prof. Dr. G. Niedner-Schatteburg

Mein besonderer Dank gilt:

Herrn Prof. Dr. Markus Gerhards für die freundliche Aufnahme in seine Arbeitsgruppe, die Vergabe des interessanten Themas, die hervorragende Betreuung sowie viele konstruktive Diskussionen. Insbesondere möchte ich mich auch für die Möglichkeit bedanken, meine Ergebnisse auf vielen Tagungen vorzustellen.

Herrn Prof. Dr. Gereon Niedner-Schatteburg für die Übernahme des Zweitgutachtens.

Herrn Prof. Dr. Jens Hartung für die Übernahme des Komissionsvorsitzes.

Andreas Funk für die Durchführung sämtlicher Rechnungen die für die Interpretation der Ergebnisse unerlässlich waren.

Dr. Holger Fricke für die detaillierte Einführung in die Apparatur und die Laser Systeme.

Kirsten Schwing für die Sorgfalt beim Korreturlesen und die stilistischen Hinweise.

Yvonne Schmitt, Philip Bialach, Martin Weiler, Andreas Funk, Holger Fricke und Kirsten Schwing für die gute Zusammenarbeit und Unterstützung bei Messungen und Diskussionen.

Rolf Linder für die Aufnahme des Absorptionsspektrums sowie die ständige Hilfs- und Diskussionsbereitschaft.

Hans-Josef Bongard aus der EM-Abteilung des Max-Planck-Instituts für Kohlenforschung für die Aufnahme des EDX-Spektrums

Herrn Priv.-Doz. Dr. Klaus Schaper sowie seiner Mitarbeiterin Daniela Maydt für die Synthese der Caged Compounds.

Herrn Prof. Dr. Hans-Dieter Martin († 08.03.2009) sowie seiner Mitarbeiterin Dr. Grit Kock für die Synthese des 2-(2-Naphtyl)-3-hydroxychromons.

Klaus Kelbert für die Hilfsbereitschaft und das Engagement bei der Lösung elektronischer Probleme.

Der Zentralwerkstatt Chemie und Physik der Heinrich-Heine-Universität Düsseldorf sowie den Zentralen Metallwerkstätten der Technischen Universität Kaiserslautern für die prompte und zuverlässige Bearbeitung vieler benötigter Spezialanfertigungen. Insbesondere sei hier der „Wagen“ für den Transport der Apparatur von Düsseldorf nach Kaiserslautern hervorgehoben.

Allen Mitarbeitern des Institutes für Physikalische und Theoretische Chemie der Technischen Universität Kaiserslautern sowie des Institutes für Physikalische Chemie I der Heinrich-Heine-Universität Düsseldorf für das gute Arbeitsklima.

Der Deutschen Forschungsgemeinschaft (DFG) für die finanzielle Unterstützung (SFB 663 und GE 961/8-1).

Besonderer Dank gilt meinen Eltern, die mir eine Universitätsausbildung so selbstverständlich erscheinen lassen haben und mich von jeher in jeder Hinsicht unterstützt haben. Ohne Euch wäre diese Arbeit nicht möglich gewesen.

Bastian Schaack danke ich von ganzem Herzen für seine unermüdliche Unterstützung, seine Geduld, sein Verständnis und seine Liebe. Danke! Des Weiteren bedanke ich mich für die konstruktive Kritik bezüglich dieser Arbeit sowie die Hilfe bei Computer Problemen.

“Denn was man messen kann,

das existiert auch.“

Max Planck

Contents

1. Introduction

This thesis is focused on the structure, energy and reactivity of excited singlet and triplet states in isolated molecules and small aggregates. In particular primary steps of elementary photoinduced reactions are investigated in isolated model systems. Thus intra- and intermolecular interactions can be identified, and a detailed understanding of these model systems makes it possible to draw conclusions concerning biomolecules in a more complex environment.

Special focus is on proton transfer reactions upon photoexcitation, which play a role for instance in excited state deactivation mechanisms: The photostability of DNA is assigned to fast internal conversion of the electronically excited state to the electronic ground state, leading to short lifetimes of the excited state and thus preventing photochemical reactions. Excited states of Watson-Crick base pairs in DNA decay via a $\pi\pi^*$ charge-transfer state which is stabilized by a proton or hydrogen transfer (cf. example [1-5]). This thesis deals with primary steps of light induced proton transfer reactions, also described as a keto-enol tautomerism. One molecule which has been investigated in this work by IR spectroscopy with regard to an excited state proton transfer reaction is 3-hydroxyflavone, a representative of flavonoids which are known for their photoprotective and antioxidative effects. Furthermore 2,5-dihydroxybenzoic acid, which is used as a matrix substance[6] in MALDI (matrix assisted laser desorption ionization) sources[7], and 2-(2-naphthyl)-3-hydroxychromone have been analyzed by IR spectroscopy concerning a possible proton transfer in the excited state.

Additionally the mono- and the dihydrate of 3-hydroxyflavone have been investigated with regard to proton wire reactions. Proton migration along solvent chains of hydrogen bonded water molecules play a major role in the energetic of cell membranes[8, 9]: Many transmembrane proteins create, control or utilize proton gradients across the biological membranes. Hydrogen bonded wires were identified for instance in the membrane spanning proteins such as bacteriarhodopsin[10-12], the bacterial photosynthetic reaction centers[13-15] and the transmembrane channel formed by gramicidin[16-18]. The proton transfer can be described by a mechanism which is similar to the proton translocation described by the Grotthus model through bulk liquid water[19, 20]. For a better understanding of these mechanisms, isolated small model systems exhibiting a proton wire

along a chain of solvent molecules were analyzed: 7-Hydroxyquinolin[21-35] and 7-azaindole[36-40] were investigated by fluorescence, UV and combined UV/UV spectroscopy with regard to an excited state proton transfer along ammonia, methanol and water wires. Although the proton transfer is confirmed for the aggregates with ammonia and methanol (whereas it did not occur for the water wires), no direct structural information about the excited states were obtained. Aggregates of 3-hydroxyflavone with water can also serve as model systems for proton wire reactions. In this work the IR spectra of the electronic ground state of the mono- and the dihydrate as well as the IR spectra of the electronically excited states of the aggregate with two water molecules are presented, yielding direct and detailed geometrical information. Due to the combination of UV and IR spectroscopy an unambiguous structural assignment is possible, and the first application subsequent to an excited state proton transfer along solvent molecules (proton wire) is shown.

Fragmentation upon photoexcitation is the second topic of this work. Caged compounds as a class of substances being able to release active components after irradiation[41] have been investigated with regard to their fragmentation pathways. They are used to insert their active components into cells: For instance cyclic adenosine monophosphate (cAMP)[42, 43] as well as adenosine triphosphate[41] were bonded to an *o*-nitrobenzylic protective group and were released in the cell by a laser pulse. 6-Nitropiperonylalcohol and 6-nitropiperonylacetate serve as model systems for this substance class. For a better understanding of the observed fragmentation pattern, 3,4-methylendioxynitrobenzene, 3,4-dimethoxynitrobenzene and 5-nitroindole have been investigated as precursor molecules.

As photochemical intra- and intermolecular reactions involve not only singlet but also triplet states[44], the analyses of those are of interest as well. Furthermore photoinduced reactions originating from triplet states are highly probable due to their long lifetimes. The energies of T_1 states can easily be determined by phosphorescence spectroscopy, including investigations in solution as well as in molecular beams. Still these analyses are often limited to the lowest triplet states and almost no information about the higher ones are obtained, which are of interest due to the fact that often more triplet states than the T_1 state are located energetically below the S_1 state (c.f. example [45]). The energy of these triplet states is accessible by photoexcitation of the anion (photoelectron spectroscopy) (cf. example [46-51]). Still no direct structural information about triplet states are obtained by either phosphorescence or photoelectron spectroscopy. Combined IR/UV spectroscopy

offers a tool to investigate triplet states with regard to their geometry in a molecular beam: The T_1 state of the pyrazine-argon complex was investigated by photodissociation spectroscopy[52]. The ion signal was obtained via direct $T_1 \leftarrow S_0$ transition with a second UV laser ionizing the molecule. The IR photon was placed after electronic excitation and prior to ionization, and a resonant vibrational excitation leads to photodissociation, that is, the loss of an Ar atom (messenger). The IR spectrum of the cluster is taken as an estimate for the spectrum of the bare molecule. In order to analyze triplet states of isolated molecules, i.e. without using a messenger molecule, UV/IR/UV spectroscopy can be applied. Due to the fact that electronic excitation often occurs to singlet states, the analysis subsequent to an *Intersystem Crossing (ISC)* is desirable. In this thesis the UV/IR/UV technique has been applied for the first time to a T_1 state; xanthone with an efficient *ISC* serves as a model system: After electronic excitation to the S_2 state *ISC* into the triplet manifold occurs offering the possibility to investigate triplet states of isolated xanthone by combined IR/UV spectroscopy. Thus direct structural information about reaction products of photoinduced reactions in triplet states can be obtained.

In general, molecular beam experiments enable the investigation of isolated, cold molecules without any influence of the environment. Furthermore, small aggregates can be analyzed in a supersonic jet by gradually adding solvent molecules like water. Conclusions concerning the interactions in solution can be derived by investigating and fully understanding small systems with a defined amount of solvent molecules.

IR/R2PI (Infrared/Resonant 2-photon ionization) spectroscopy can be applied to electronic ground states to determine and discriminate between different structures[53-57]. IR laser systems are necessary for the application of this method in different spectral ranges: The IR light is generated by various techniques, including difference frequency mixing (DFM)[53], optical parametric oscillating (OPO)[58], DFM followed by an optical parametrical amplification (OPA) and a second DFM process[59, 60] as well as free electron lasers[61]. The first molecule analyzed with IR/R2PI spectroscopy is benzene and its dimer in the range of 3000 – 3100 cm^{-1} yielding information on the CH stretching vibrations[53]. In the case of fluorobenzene$(methanol)_n$ (n=1,2)[54] the spectral range was extended to 1020 – 1060 cm^{-1} allowing the analysis of the C-O stretching and C-H bending vibrations. The IR light was generated by a CO_2 laser. Furthermore the OH stretching vibrations of phenol$(H_2O)_n$ (n=1-3)[55] were analyzed by IR/R2PI spectroscopy in the range of 3000 – 3800 cm^{-1}. The spectral region of the C=O stretching vibrations was also accessible with

high resolution and higher power; signal and idler of an OPA (optical parametrical amplification) process are the input of a difference frequency mixing process in an $AgGaSe_2$ crystal[60]. A detailed description of the laser system including the resulting output energies as well as the obtained resolution is given in Chapter 2.3. Thus the protected amino acid AcPheOMe was analyzed in the spectral range of 1450 – 1800 cm^{-1} yielding information on the structure sensitive C=O stretching vibrations[57]. Finally the IR spectra of tryptophan were recorded in the fingerprint region of 330 – 1500 cm^{-1}[62] by using a free electron laser. The spectral range was further extended to 150 – 2000 cm^{-1} for the hydrated aggregates of tryptophan[63].

Electronically excited states can be analyzed by for instance R2PI (resonant 2-photon ionization) spectroscopy[64-66]: The first UV photon populates different vibrational levels of the excited state. Thus by scanning the UV laser, a vibrational spectrum of the excited state is obtained. In most cases only low frequencies are observed due to unfavourable Franck-Condon factors for the high frequencies. The spectrum can be attributable to one or to an overlay of different isomers with similar excitation energies (for further details cf. Chapter 2.2.1). To discriminate between different isomers, UV/UV hole burning spectroscopy[67] can be applied (cf. Chapter 2.2.3).

Furthermore combined IR/UV spectroscopy can also be applied to electronically excited states, yielding information on high frequency vibrations and thus detailed information on geometry changes upon photoexcitation[68-72]. In the first applications the IR spectrum was recorded via a decrease of the fluorescence signal (IR/fluorescence spectroscopy): The IR spectrum of propynol[70] was recorded in the range of 3250 – 3400 cm^{-1}. Furthermore the IR spectra of microsolvated aggregates of phenol, phenol$(H_2O)_n$ (n=1, 3), were recorded in the range of 3000 – 3800 cm^{-1}, yielding information on the OH stretching vibrations[71]. Additionally the IR spectrum can be detected via a decrease of the ion signal (IR/R2PI (UV/IR/UV) spectroscopy). This technique was applied to aminophtalimides and their aggregates with one and two water molecules[68] in the range of 3100 – 3800 cm^{-1}, yielding information on the NH and OH stretching vibrations. Additionally IR spectra of the electronically excited states of coumarins such as coumarin 151, coumarin 120 and coumarin 152A and its aggregates with acetonitrile, water and acetone[69] were recorded in the range of 3000 – 3800 cm^{-1} by IR/R2PI spectroscopy, yielding information on the NH and OH stretching vibrations.

By setting the second UV photon to the exact ionization potential, a triple resonance technique, IR/MATI (IR/mass analyzed threshold ionization) spectroscopy, can be applied to electronically excited states; resorcinol was investigated with this technique in the range of 3520 – 3700 cm^{-1} yielding information on the OH stretching vibrations[72].

Thus the mass and isomer selective IR/R2PI method can be applied to electronic ground as well as to electronically excited singlet states. Besides the structure in different neutral states, the ionic states are of interest as well: By applying the IR/PIRI (IR/photo induced Rydberg ionization) triple resonance technique[72], the ionic states of molecules can be analyzed. A detailed description of the spectroscopic techniques is given in Chapter 2.2.

Structural assignments of the different electronic and ionic states are derived by comparing the IR spectra with *ab initio* and (TD)DFT calculations[73]. Therefore geometry changes upon photoexcitation can be identified and detailed structural information about the reaction products can be obtained.

In this work new variants of IR/UV double and triple resonance techniques are introduced: IR/PIRI spectroscopy has been applied for the first time in the region of the C=O stretching vibrations of 2,5-dihydroxybenzoic acid. Also a new variant of combined IR/UV spectroscopy has been introduced in the region of the C=O stretching vibrations in the excited state of 2,5-dihydroxybenzoic acid. Finally the first application of the IR/UV double resonance technique to excited triplet states without any messenger molecules subsequent to an *Intersystem Crossing* is shown in this work. Furthermore, the IR/R2PI technique has also been introduced subsequent to reactions - in this case a proton transfer reaction - in the excited state of 3-hydroxyflavone and its aggregate with two water molecules. In the case of the dihydrate, the proton transfer reaction along the water molecules (proton wire) has to be induced by raising the excitation energy. Altogether it is shown that IR/UV double and triple resonance techniques are suitable tools to analyze reaction coordinates of photochemical processes.

The results are summarized in Chapter 3 and the associated publications are attached.

2. Apparatus and Spectroscopic Techniques

All experimental results presented in Chapter 3 have been obtained in molecular beam experiments on isolated molecules and their aggregates with water. Spectroscopic methods are combined with mass spectrometry, leading to mass resolved spectra. The apparatus in which the experiments have been carried out, the various - partly new - spectroscopic techniques which have been applied as well as the laser systems used to generate the necessary UV and IR radiation are described in this chapter.

2.1 Apparatus

The high vacuum apparatus consists of three differentially pumped vacuum chambers (Figure 2.1). The first chamber is evacuated by a diffusion pump (3000 l/h, DI 3000, Leybold); a rotary vane pump (65 m^3/h, Alcatel) and a roots pump (250 m^3/h, Alcatel) serve as forepumps. A pressure of $8*10^{-6}$ mbar is achieved as long as the pulse valve is closed, it is degraded to about $3*10^{-4}$ mbar in the operating mode. The substance is placed in a glass crucible in a steel sample storage comprised in the first chamber. The sample storage consists of two cylindrical micro chambers that are connected by a steel tube and can be heated individually up to 220 °C (Figure 2.2). The sample storage is clamped in a device which can be adjusted in six dimensions from the outside: The translation into the three spatial directions, the rotation in two different planes and the rotation of the front flange of the pulse valve.

The micro chambers are filled with the substance (either one or two samples) which are transported to the front flange by a carrier gas (p = 2 - 3 bar, either helium or neon). Finally the molecules are expanded into vacuum by the pulse valve (Iota One, General Valve, orifice: 500 µm). The valve can be heated up to 220 °C as well.

The molecular beam enters through a skimmer (Beam Dynamics, aperture 1 mm) into the second chamber. This chamber is evacuated by a turbomolecular pump (Turbovac1000, Leybold), which is affiliated to the same forepumps as for the first chamber. A pressure of $2*10^{-7}$ mbar is achieved in the operating mode (pulse valve on). The supersonic jet is

crossed perpendicularly by up to three laser beams in the second chamber. The ionized molecules pass on for 3 cm without applying any electric field, or - in the case of MATI[74] or IR/PIRI[72] experiments - with a small electric field (1-2 V/cm). Thus, ions which do not result from ionization of the molecular beam are suppressed. Afterwards a pulsed high voltage accelerates the ions perpendicularly towards the detector; or - in the case of MATI[74] and IR/PIRI[72] experiments - the Rydberg neutrals are ionized and accelerated.

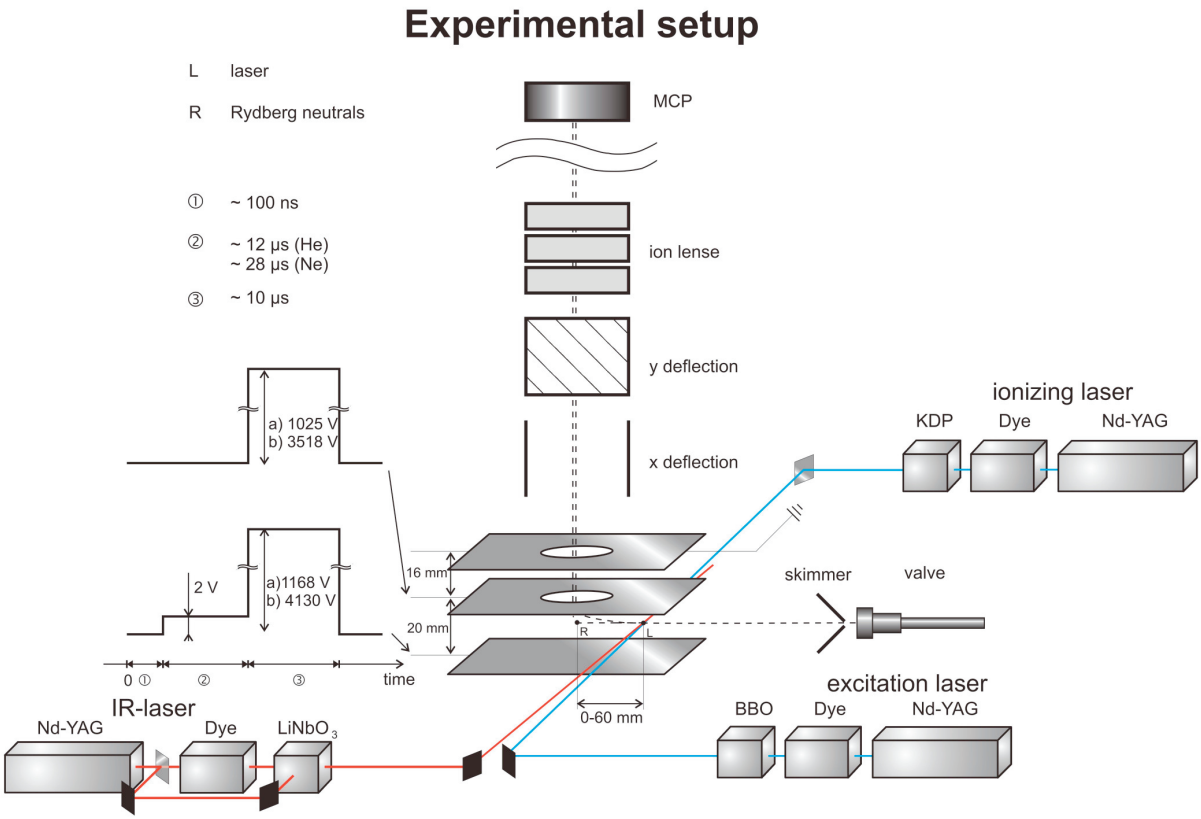

Figure 2.1: Apparatus including the ionizing and excitation laser as well as the IR laser. The applied voltages of the acceleration plates differ depending on the molecule: In the case of DHB a set of 1168 V and 1025 V has been used, for the other molecules a set of 4130 V and 3518 V has been applied (cf. Appendix A).

The third chamber is the time-of-flight mass spectrometer. This chamber is evacuated by a turbomolecular pump (Turbovac361, Leybold), whereas a rotary vane pump (8 m^3/h, Leybold) serves as forepump. A pressure of $2*10^{-8}$ mbar is achieved in the operating mode.

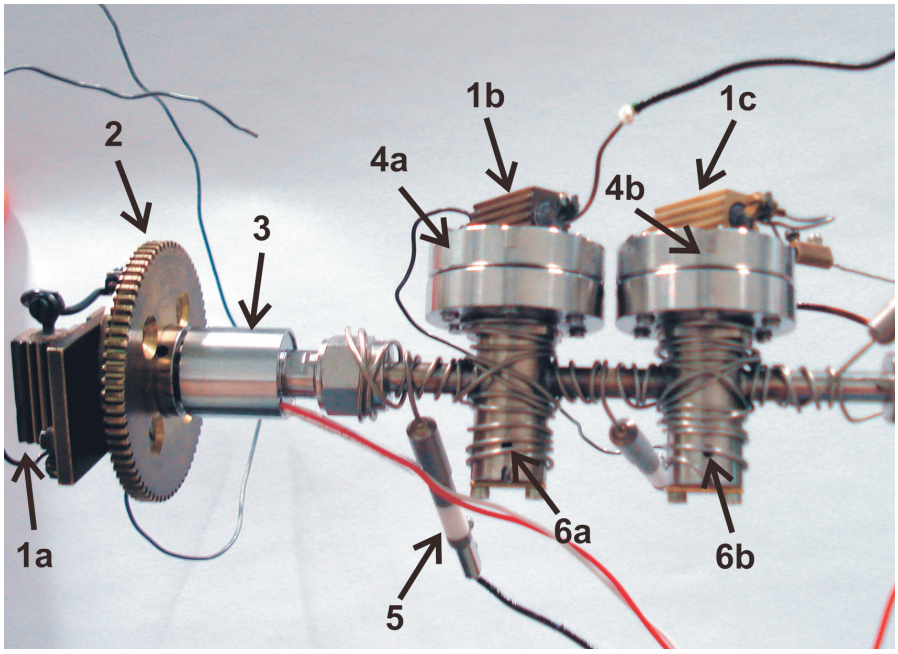

Figure 2.2: Sample storage including the pulse valve:

1) Resistances for thermalization of a) the front flange of the pulse valve, of b) the first and of c) the second micro chamber. The pulse valve (3) is clamped by a connector made of brass, which is also heated by resistances and connected to (1a). The pulse valve has the highest temperature, followed by the first micro chamber. Thus the molecules are transported by the carrier gas towards slightly higher temperatures and precipitation is circumvented.

2) Cogwheel, part of the arrangement to rotate the front flange.

3) Pulse valve (Iota One, General Valve, orifice: 500 µm).

4) ConFlat flange (CF 16) for a) the first and b) the second micro chamber. The arrangement of two chambers allows the investigation of either one substance (first chamber) but also of two substances for e.g. mixed dimers. For two samples the one requiring higher temperatures is placed in the first micro chamber.

5) Heating element (Thermocoax), two of them are wrapped around the sample storage to heat the system.

6) Drills for thermocouples to control the temperature. A third temperature receiving device is used to control the temperature of the connector clamping the pulse valve.

In order to obtain a Wiley-McLaren arrangement[75], three deflection plates are used (two acceleration fields instead of one). The advantage of this arrangement is that ions of the same mass but with different points of origin are focused by the first acceleration field. Thus the ions are focused temporally, i.e. arrive at the same time at the detector. A resolution of $m/\Delta m = 1800$ for a mass of 110 Da can be achieved. Additionally deflection

voltages in x- and y-direction can optimize the flight route. Three voltages are connected to the microchannel plate detector in chevron arrangement:

VD1 = 0 to -2200 V

VD2 = 0 to -1200 V (54.5 % of VD1) and

VD3= 0 to -200 V (9.1 % of VD1).

For the experiments in this thesis voltages of -1700 V (VD1) and therefore -926.5 V (VD2) as well as -154.7 V (VD3) have been applied, leading to a voltage level of about 770 V for each of the two microchannel plates (amplification: 10^6). The resulting electron current is further amplified by a wideband voltage amplifier (HVA-200M-40-B, 40 dB, Femto) before being visualized on a digital oscilloscope (TDS 520, Techtronics).

The apparatus is pulsed operated (10 Hz): The timing of the various lasers and the pulse for the acceleration voltage is controlled by two Digital Delay/Pulse Generators (DG 535, Stanford Research and a self-made one) which are triggered by the pulse driver (Iota One, General Valve) for the pulse valve. For a detailed description cf. Appendix B.

2.2 Spectroscopic Techniques

2.2.1 Resonant Two-Photon Ionization[64-66]

The cations of the investigated molecules result from a resonant two-photon ionization (R2PI). The first UV photon populates different vibrational levels of the electronically excited state; the second UV photon ionizes the molecule (Figure 2.3a). In the case of a resonant excitation, the ion signal is considerably larger than in the case of a non resonant excitation. Thus, by scanning the first UV laser, a vibrational spectrum of the excited state is obtained. In most cases only low frequencies are observed due to unfavourable Franck-Condon factors for the high frequencies. This spectrum can be attributable to one isomer or to different isomers with similar excitation energies. For combined UV/UV and IR/UV spectroscopic techniques to discriminate between different isomers cf. Chapter 2.2.2 and Chapter 2.2.3.

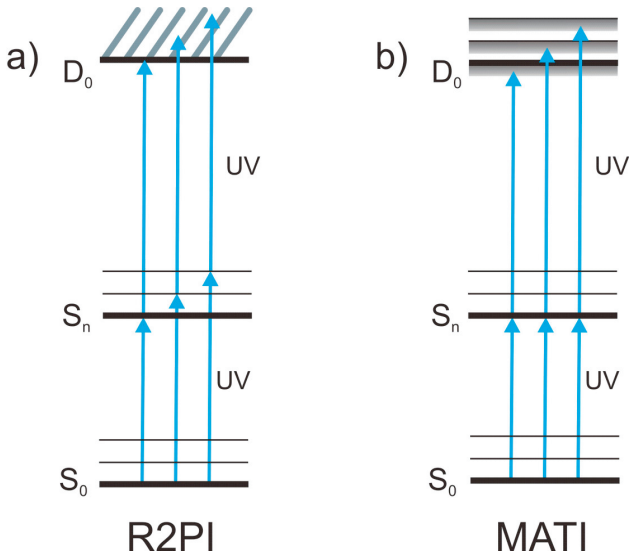

Figure 2.3: Scheme illustrating a) R2PI and b) MATI spectroscopy

a) The excitation laser is scanned; in the case of a resonant excitation the ion signal is considerably larger than in the non resonant case. Thus a vibrational spectrum of the excited state is obtained.

b) The ionizing laser is scanned while the excitation laser is set to a resonant transition. Rydberg states which are located directly below the ionization potential and the vibronic levels of the cation can be seperated from the direct ions. An isomer selective spectrum of the ionic state is obtained.

After photoexcitation to the S_1 state, a UV photon of the same wavelength can be used for ionization, which is called one-color R2PI. If a UV photon of a different wavelength is used to ionize the molecule, it is called two-color R2PI. If the energetic distance between the S_0 and the electronically excited state is shorter than the distance between the excited and the ionic state, it is inevitable to use a UV photon that is sufficient to exceed the ionization potential. It might also be useful to use a UV photon with a longer wavelength in cases where the exciting photon can easily exceed the ionization potential to prevent fragmentation in the ionic state. In this work all R2PI spectra - except for the caged compounds - have been recorded with a second UV photon of a shorter wavelength in order to exceed the ionization potential.

Ion Current Spectrum

By scanning the second UV laser, while the first laser is fixed on a resonant transition, the ion current of the molecule can be recorded. If the energy of the second UV photon exceeds the ionization potential, a steep raise of the ion current is observed. The ionization potential is exceeded at the point of inflection and thus the ionization potential can be determined by setting a tangent to it. A more accurate value for the ionization potential can be obtained by recording a MATI spectrum[74] (cf. Chapter 2.2.2), which corresponds to the first derivative of the ion current. Additional steps can occur in the ion current spectrum in the case of a resonant excitation to a vibrational level of the ionic state. These are often not well resolved, MATI spectra provide a better resolution (cf. Chapter 2.2.2). Thus a vibrational spectrum of the ion is obtained which is attributable to only one isomer due to the isomer selective excitation to the S_1 state.

2.2.2 Mass Analyzed Threshold Ionization[74]

To obtain a more accurate value for the ionization potential, mass analyzed threshold ionization (MATI)[74] spectroscopy is applied. MATI spectroscopy is similar to the pulsed field ionization - zero kinetic energy (PFI-ZEKE)[76-79] method. Both techniques are based

on the field ionization of long living Rydberg states which are located directly below the ionization potential and the vibronic levels of the cation. The first UV laser is fixed to a resonant transition, while the second laser is scanned (Figure 2.3b). The laser pulse generates Rydberg neutrals as well as direct electrons (and ions). The Rydberg neutrals are separated from the direct electrons by an electric field which is switched on 100 ns after the two UV lasers crossed the probe volume. Afterwards a strong electric field is applied, the ionization potential is lowered and thus the Rydberg neutrals are ionized. The resulting electrons are accelerated towards a detector and can be analyzed.

In order to obtain a mass resolution, the resulting ions can be detected by using time-of-flight mass spectrometry. As the mass of the direct ions is much larger than the one of the electrons, a stronger electric field of 1-2 V/cm has to be applied to separate these from the Rydberg neutrals. This leads to field ionization of more Rydberg neutrals even before the strong electric field for ionization and acceleration towards the detector is applied. Thus the signal of the field ionized Rydberg neutrals is less intense compared to the one of the electrons.

The obtained ionization potentials have to be corrected by the electric field used to separate the two species: By applying the electric field, Rydberg states of the same quantum number are shifted and split into Stark states. Due to the high density of the Rydberg states, the resulting Stark states of different main quantum numbers can cross. If the electric field rises slowly, avoided crossings have to be taken into account, which is called adiabatic ionization. In the case of a fast rising electric field these crossings are still avoided which is called diabatic ionization. The subsidence of the ionization potential depends on the electric field which is applied and thus the obtained value has to be corrected by

$$4*\sqrt{F}\ (V*cm)^{-1}$$

in the case of a diabatic ionization and by

$$6*\sqrt{F}\ (V*cm)^{-1}$$

in the case of an adiabatic ionization[80-82]. For the experiments described in this work the diabatic ionization is applied.

By scanning the ionizing laser, a vibrational spectrum of the ionic state is obtained via the ion signal resulting from the Rydberg neutrals. In contrast to the R2PI spectrum of the excited neutral state, this spectrum is attributable to only one isomer as the first resonant excitation is isomer selective.

2.2.3 Combined Infrared/Ultraviolet Spectroscopy[53-57, 68-72, 83, 84]

Various combined IR/UV techniques can be applied to electronic ground and electronically excited states in molecular beam experiments.

For the Infrared/Resonant 2-photon ionization (IR/R2PI)[53-57] method, the excitation laser is fixed to one transition of the R2PI spectrum and the ionizing laser is set above the corresponding ionization potential. This leads to a constant ion signal. The IR photon arrives prior to the first UV photon, and in the case of a resonant vibrational excitation, the vibrational ground state of the S_0 state is depopulated, leading to a decrease of the ion signal[53-57] (Figure 2.4a). By scanning the IR laser an IR/R2PI spectrum of one isomer - due to the isomer selective excitation - of the electronic ground state is obtained and different transitions of the R2PI spectrum can be assigned to the corresponding isomers.

The IR spectrum in the case of IR/MATI spectroscopy[72] is also recorded via a depletion of an ion signal. In contrast to the IR/R2PI technique, the ionizing laser excites the molecule to long living Rydberg states (cf. Chapter 2.2.2) and the IR spectrum is recorded via a decrease of the ion signal of the field ionized Rydberg neutrals (Figure 2.4b).

A technique that differs only in the detecting method is IR/fluorescence spectroscopy[56, 83, 84]: Instead of a decrease of the ion signal, the fluorescence of the excited state is detected. The IR photon arrives prior to the UV photon, and in the case of a resonant vibrational excitation, the vibrational ground state of the electronic ground state is depopulated leading to a less efficient excitation to the excited state and thus to a decrease of the detected fluorescence (Figure 2.4c).

Both detection methods yield the same IR spectra, in the case of the IR/R2PI and the IR/MATI spectroscopy the analysis is mass resolved. This is not the case for

IR/fluorescence spectroscopy, but on the other hand only one UV photon is required to record the IR spectrum. Due to the choice of nanosecond lasers, IR/R2PI spectroscopy requires lifetimes on a nanosecond timescale of the excited state as ionization occurs from thereon.

If the electronic transitions of two isomers are overlaid, combined IR/UV methods fail to discriminate the isomers: The recorded IR spectrum can be due to an overlay of different isomers. To assign the obtained transitions to the corresponding structures, IR/IR/UV hole burning spectroscopy[85] can be applied (Figure 2.4d): The first IR laser is set to a vibrational transition, the second IR laser is scanned. All bands belonging to the same species as the one depopulated by the first IR laser will be considerably less intensive in the IR spectrum. Thus by comparing the IR spectrum obtained by IR/UV spectroscopy to the one recorded by the IR/IR/UV technique, vibrational transitions of one isomer can be identified. This technique requires two IR photons and thus two IR laser systems are necessary.

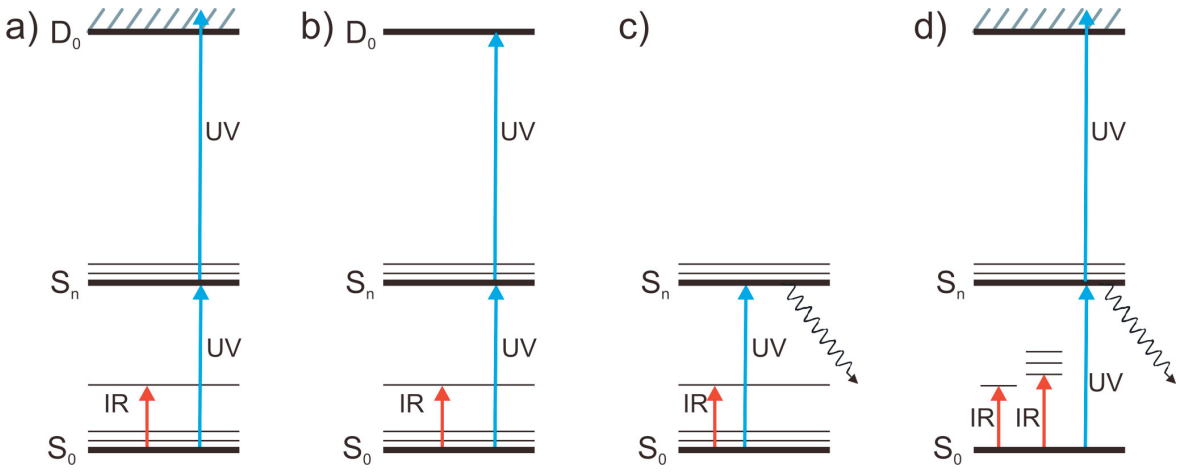

Figure 2.4: Schemes illustrating different IR techniques for the electronic ground state:

a) IR/R2PI spectroscopy for the electronic ground state.

b) IR/MATI spectroscopy for the electronic ground state.

c) IR/fluorescence spectroscopy for the electronic ground state.

d) IR/IR/UV hole burning spectroscopy for the electronic ground state. The IR spectrum can either be recorded via the depletion of the fluorescence signal of the S_1 state or via the depletion of the ion signal of the R2PI process.

All techniques can also be applied to electronically excited states: For IR/fluorescence spectroscopy[70, 71] the IR photon arrives temporally after the UV photon. In the case of a resonant vibrational excitation in the excited state, the fluorescence decreases due to a depopulation of the vibrational ground state of the electronically excited state (Figure2.5a).

The spectrum of the excited state can also be detected via a decrease of the ion signal of the R2PI process (IR/R2PI)[68, 69]: Therefore the IR photon arrives temporally in between the first and the second UV photon (UV/IR/UV spectroscopy). In the case of a resonant vibrational excitation, the ion signal decreases (Figure 2.5b). IR/MATI spectroscopy[72] can also be applied to electronically excited states: The ionizing laser excites the molecule to long living Rydberg states (cf. Chapter 2.2.2) and the IR spectrum is recorded via a decrease of the ion signal of the field ionized Rydberg neutrals (Figure 2.5c). For this technique two isomer selective steps are applied: the electronic excitation to the excited state and the ionization from thereon, but it requires the possibility to record MATI spectra of the molecule (cf. Chapter 2.2.2).

In this thesis the IR/R2PI method (UV/IR/UV) has been applied subsequent to a proton transfer reaction in the excited state (Figure 2.5d): After vertical excitation to the short lived S_1 state, an excited state proton transfer occurs, leading to a second deeper minimum called S'_1 state. By placing the IR photon temporally between the proton transfer reaction and the ionizing UV photon, the IR spectrum of the tautomeric form is recorded. The obtained spectra are depicted in the attached ref. [II] and [III]. Furthermore IR/R2PI spectroscopy (UV/IR/UV) has been applied for the first time to a triplet state subsequent to an *Intersystem Crossing* (*ISC*) in this work (Figure 2.5d): A molecule which exhibits an efficient *ISC* is excited to its electronically excited singlet state (in this thesis the S_2 state), followed by *ISC*, leading to the triplet manifold. By placing the IR photon temporally between the *ISC* and the ionizing UV photon, a spectrum of the triplet state can be recorded. The obtained spectrum is depicted in the attached ref. [IV].

In this thesis another variant of IR/R2PI spectroscopy for electronically excited states, the UV+(IR+UV) method, has been applied successfully in the region of the C=O stretching vibrations for the first time: The ionizing laser is set to a wavelength so that the sum of excitation and ionizing laser is not sufficient to ionize the molecule. By scanning the IR laser to vibrational levels of the excited state of the molecule, the sum of three photons (UV+IR+UV) exceeds the ionization potential and an ion signal is obtained (Figure 2.5e). This method allows measuring against a zero base line since neither an

excitation with two UV1 photons nor the sum of UV1 and UV2 photon leads to an ion signal. (The non resonant excitation and ionization with two UV2 photons is also not efficient enough to form an ion signal.) Thus the signal to noise ratio is excellent which allows observing small effects. The recorded spectrum is depicted in the attached ref. [I] and in Figure 3.4.

All techniques presented here have in common, that they are isomer and structure selective. Another approach to discriminate between different isomers, which is not structure selective, is the application of combined UV/UV spectroscopy: For UV/UV hole burning spectroscopy[67], one UV laser (probe laser) is set to a transition of the R2PI spectrum, leading to a constant ion signal. Then a second UV laser (burn laser) is scanned over the complete range of the R2PI spectrum, arriving approximately 150 ns prior to the probe laser. If the burn laser is in resonance with a transition that shares the same electronic ground state with the species which is excited by the probe laser, the S_0 state is depopulated leading to a decrease of the probe signal. Thus the obtained spectrum exhibits bands which belong to only one isomer.

Another combined UV/UV technique which can be applied is MATI spectroscopy (cf. Chapter 2.2.2): The first UV photon is set to one transition of the R2PI spectrum (cf. Chapter 2.2.1) while the second one is scanned. Thus different isomers can be distinguished by their exact ionization potentials.

In order to record an IR spectrum of the ion, the infrared/photo induced Rydberg ionization (IR/PIRI)[72] spectroscopy is applied: In this triple resonance technique, the excitation laser is set to one transition of the R2PI spectrum and the ionizing laser is fixed to a high lying Rydberg state converging to the ionization potential (cf. Chapter 2.2.2). The IR photon arrives after the second UV photon. In the case of a resonant vibrational excitation, autoionization of the Rydberg state occurs, leading to a decrease of the ion signal arising from the Rydberg neutrals (Figure 2.4f), i.e. a decrease of the MATI signal (increase of the ion signal of the direct ions). The obtained IR/PIRI spectrum is attributable to one isomer in the ionic state due to the isomer selective excitation.

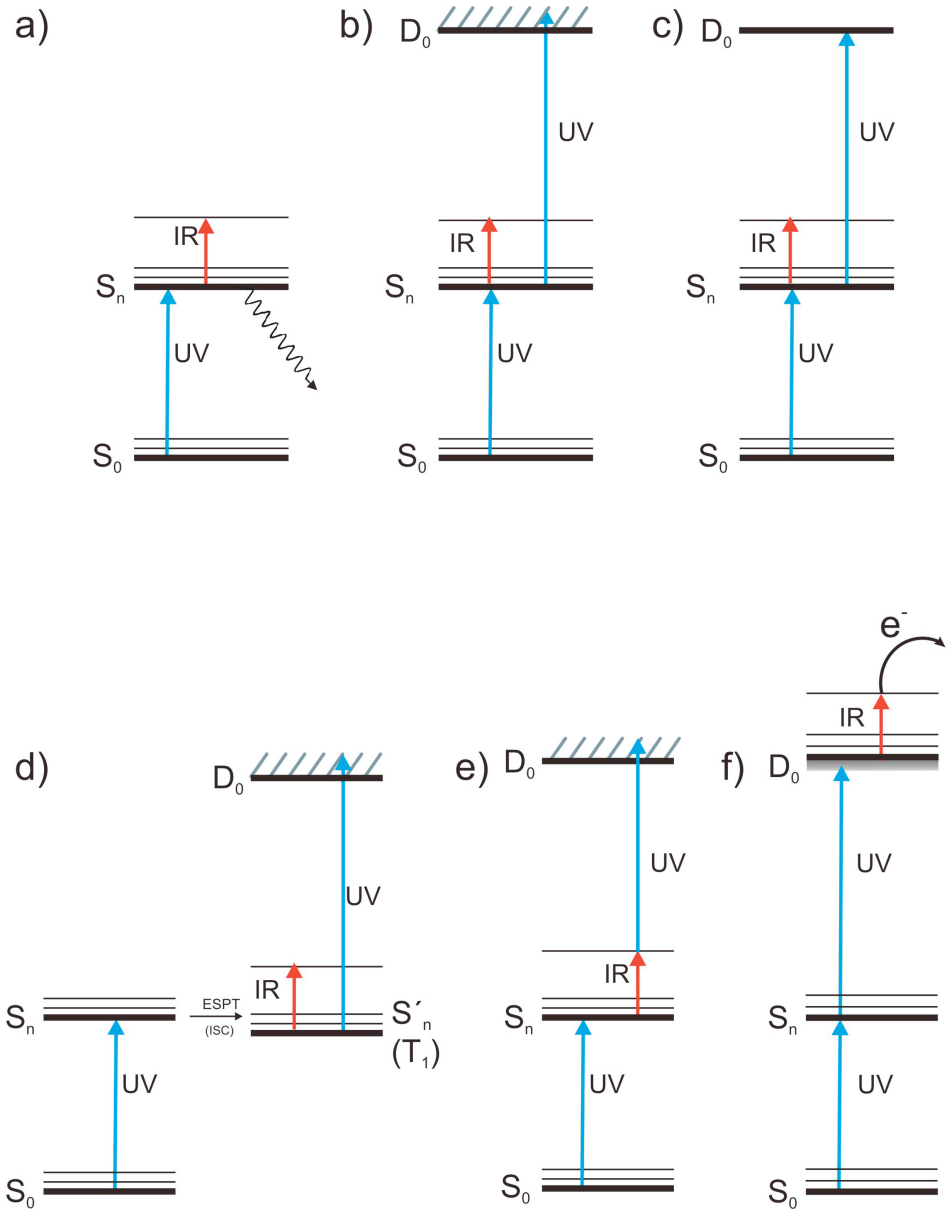

Figure 2.5: Schemes illustrating different IR techniques for electronically excited states and the ionic state:

a) IR/fluorescence spectroscopy for the electronically excited state

b) IR/R2PI spectroscopy for the electronically excited state

c) IR/MATI spectroscopy for the electronically excited state

d) IR/R2PI spectroscopy subsequent to an excited state proton transfer and an *Intersystem Crossing*

e) UV+(IR+UV) spectroscopy for the electronically excited state

f) IR/PIRI spectroscopy.

2.3 Laser Systems

Two Nd:YAG lasers (Lumonics HY 400 and Lumonics HY 750) are used to pump two dye lasers with the second (Lumonics HD 300 and Sirah Cobra-Stretch) or the third harmonic (Lumonics HY 750 and Sirah Cobra-Stretch). The output of the Dye laser is then frequency doubled in a crystal (KDP or BBO, depending on the wavelength).

The IR radiation results from consecutive non-linear processes (Figure 2.6). The IR light in the region of 2600 - 4200 cm^{-1} is generated with a $LiNbO_3$ crystal by difference frequency mixing (DFM) of the fundamental (1064 nm) of a seeded Nd:YAG laser (Spectra-Physics PRO-230) and the output of a dye laser (Sirah, Precision Scan) pumped by the second harmonic (532 nm) of the same Nd:YAG laser. The Dye laser is used in the range of 735 - 833 nm (Styryl 8 and Styryl 9), and the DFM process is generated in a $LiNbO_3$ crystal with a length of 30 mm. The crystal is doped with MgO in order to increase the damage threshold. The incoming beams are separated from the IR pulse by two dichroic mirrors before the output is amplified by mixing it with the fundamental of the Nd:YAG laser in a second $LiNbO_3$ crystal with a length of 50 mm. Two photons result from this OPA (optical parametrical amplification): One with the same wavelength as the IR input (idler) and one in the range of 5200 - 6800 cm^{-1} (signal). The remaining radiation of fundamental and signal is separated from the idler by two dichroic mirrors. In order to obtain an overall output (signal and idler) of 48 mJ, a dye input of 30 mJ and energies of 150 mJ and 240 mJ at 1064 nm are used for the DFM and OPA process. At 4700 cm^{-1} the output is equally distributed to signal and idler, at a wavenumber of 3689 cm^{-1}, the idler pulse has an energy of about 18 mJ. The resolution in this region is < 0.04 cm^{-1}. Due to self-absorption of the $LiNbO_3$ crystals, the range of 3460 - 3520 cm^{-1} is not accessible with these crystals. Therefore another $LiNbO_3$ crystal differing in the MgO endowment is used for the DFM process. The exact Mg endowment was determined by energy dispersive x-ray spectroscopy (EDX) to be 6 atomic percent (Figure 2.7). The self-absorption of this crystal is in the range of 3520 - 3550 cm^{-1}. The dye input is raised to 60 mJ and the obtained IR pulse with an energy of 5 mJ is used without further amplification in this range.

The IR light in the region of 1000 - 1800 cm^{-1} is generated in a third nonlinear process[57, 60]: Signal (5200 - 5600 cm^{-1}) and idler (3800 - 4200 cm^{-1}) of the OPA process

are the input of a difference frequency mixing process in an $AgGaSe_2$ crystal with a length of 18 mm leading to the IR light of 1000 - 1800 cm^{-1}. The remaining radiation of signal and idler is separated from the mid IR pulse by two dichroic mirrors. With an overall input of signal and idler of 15 mJ, the resulting output at 1645 cm^{-1} and 1200 cm^{-1} is 440 µJ and 380 µJ respectively. The resolution is < 0.1 cm^{-1} in this region. Due to the effective surface and the specified input power for the $AgGaSe_2$ crystal, the overall input of signal and idler could be raised up to 50 mJ. The pulse energy of the IR light has been determined at 1645 cm^{-1} with respect to the total input energy in the range of 6 mJ to 15 mJ. By an extrapolation of this curve pulse energies of 2 mJ are predicted for input energies of 40 mJ. For further details see ref. [60].

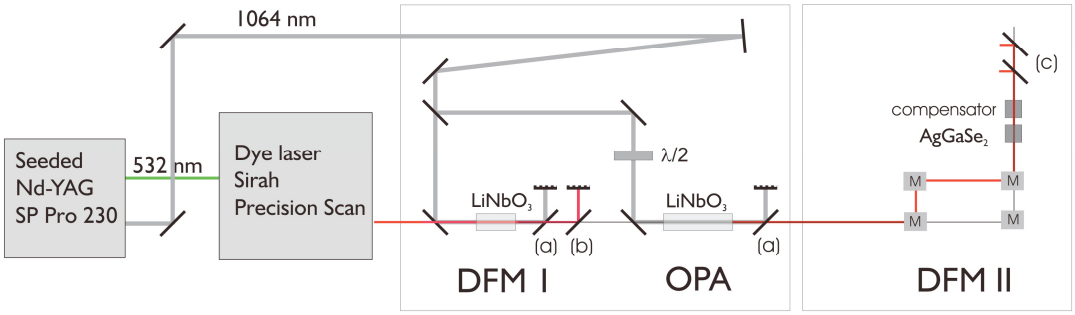

Figure 2.6: Scheme illustrating the IR laser system[60].

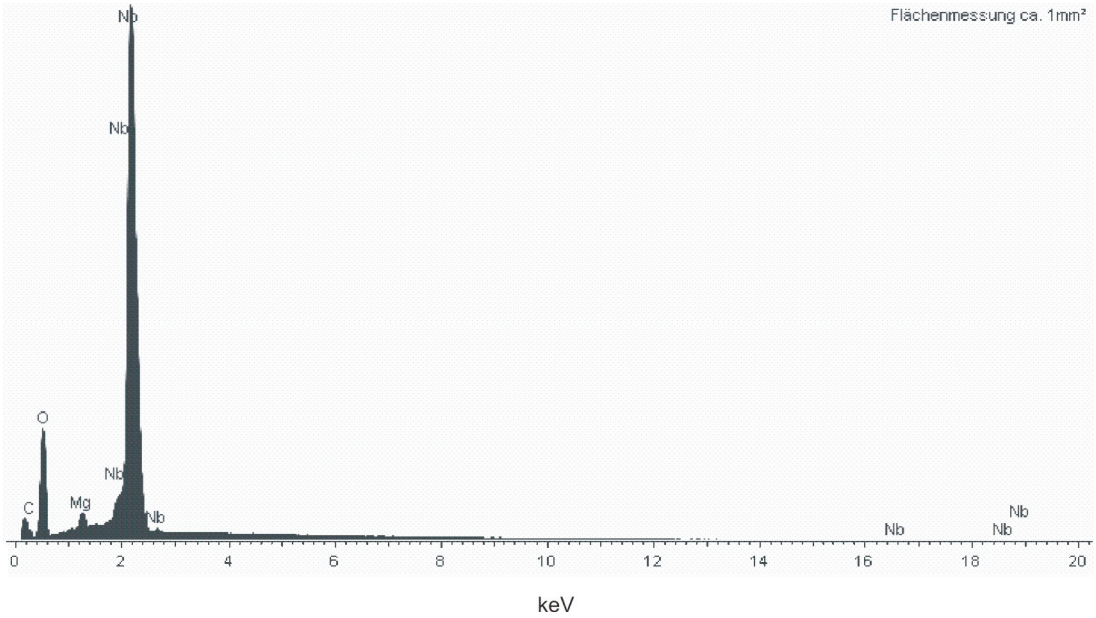

Figure 2.7: EDX spectrum (EDX, Oxford Instruments, attached to Hitachi S-3500 scanning electron microscope) of the $LiNbO_3$ crystal used in the range of 3400 - 3520 cm^{-1}, yielding an endowment of 6 % Mg.

3. Results and Discussion

Primary steps of photoinduced reactions, including excited state proton transfer reactions as well as fragmentation pathways, have been investigated in this thesis: Direct information on structures and reaction pathways of isolated molecules and their aggregates with water have been obtained by applying combined IR/UV spectroscopy.

3-Hydroxyflavone (3-HF), 2-(2-naphthyl)-3-hydroxychromone (2-NHC) and 2,5-dihydroxybenzoic acid (DHB) have been analyzed with regard to an excited state proton transfer reaction. Furthermore the dihydrate of 3-HF has been investigated with respect to a proton or hydrogen transfer along a solvent wire as the water molecules can be inserted between the hydroxyl and the carbonyl group. In the case of the caged compounds fragmentation pathways, requiring e.g. rearrangements in the excited state have been analyzed. Furthermore 3,4-methylendioxynitrobenzene, 3,4-dimethoxynitrobenzene and 5-nitroindole were investigated with regard to the influence of the substituent in *m*- and *p*-position onto the stability of the nitro aromatic compound. Finally xanthone has been chosen as an archetype molecule to extend combined IR/UV spectroscopy to triplet states subsequent to an *Intersystem Crossing (ISC)*. The corresponding publications are attached and are summarized in the following chapter.

3.1 2,5-Dihydroxybenzoic Acid

2,5-Dihydroxybenzoic acid (Figure 3.1) is a derivative of salicylic acid, representing a beta hydroxyl acid in which the OH group is adjacent to the carboxyl group. The vicinal position of the carboxyl to the hydroxyl group leads to a strong intramolecular hydrogen bond. Therefore salicylic acid is a model system for a possible proton transfer from the OH group to the carboxyl group in the excited state. It was first investigated by Weller, who proposed a double minimum potential along the reaction coordinate in the S_1 state[86-88]. Fluorescence and combined IR/fluorescence spectroscopy in a supersonic jet in combination with calculations provided evidence for a hydrogen dislocation rather than an excited state proton transfer upon photoexcitation[89-97]. The IR spectra were recorded for

the electronic ground state as well as for the electronically excited state in the spectral region of the OH stretching modes. All observed isomers form a hydrogen bond between the hydroxyl and the carboxyl group. The phenolic hydrogen bonded OH stretching vibration was not observed in the electronically excited state, thus it is either to broad or shifted below the investigated spectral region[90, 91]. Analyses of the methoxy derivative of salicylic acid, 5-methoxysalicylic acid, yielded the same information: No excited state proton transfer but a hydrogen dislocation was assigned[91, 97, 98].

Anthranylic acid is another molecule which is of interest concerning excited state proton transfer reactions. Compared to salicylic acid, the hydroxyl group is substituted by an amino group. Thus a hydrogen bond is formed to the carboxylic group, which is weaker than in salicylic acid. The electronic ground state and the electronically excited state were investigated by IR/fluorescence spectroscopy in a supersonic jet[99-101]: The NH stretching vibration is red shifted upon electronic excitation, investigations in the range of 1400 cm^{-1}-1800 cm^{-1} yield an assumption for the C=O stretching vibration in the excited state[101]. Analogue to salicylic acid a hydrogen dislocation rather than a proton transfer was observed. This assignment is confirmed by calculations (TDDFT/B3LYP/cc-pVDZ) of Sobolewski and Domcke[94].

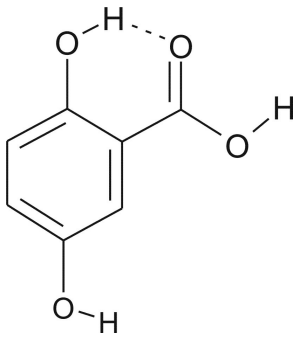

Figure 3.1: 2,5 Dihydroxybenzoic acid (DHB).

DHB (Figure 3.1) is important as a matrix substance[6] in MALDI (matrix assisted laser desorption ionization)[7] sources. In order to find out whether protonation in the MALDI process is induced by an excited state proton transfer, the laser induced fluorescence spectrum of DHB was recorded in a supersonic jet[102, 103]. No excited state proton transfer was observed. Still no structural assignments for the S_0, S_1 and the ionic state were obtained, and combined IR/UV spectroscopy offers an ideal tool to obtain

detailed information on the proton transfer coordinate in these states by applying it to vibrational modes which are directly involved in the hydrogen bond, i.e. the OH stretching vibration and the C=O stretching vibration have to be taken into account. In contrast to the OH stretching vibration, the C=O stretching mode can be observed in all electronic states.

3.1.1 Results for DHB [I]

Due to different orientations of the three hydroxyl groups and the carboxyl group, DHB has 16 possible isomers (Figure 3.2). In order to obtain a structural assignment, combined IR/UV spectroscopic techniques have been applied to the electronic ground state, to the electronically excited state as well as to the ionic state.

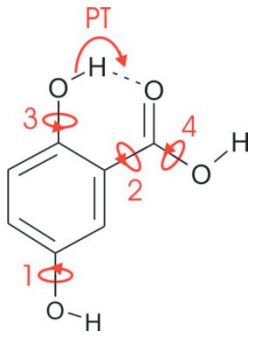

Figure 3.2: Possible rotations of the three CO and the CC bond yielding new isomers.

Initially the two-color R2PI spectrum of DHB has been recorded in the range of 27500 - 28400 cm^{-1}. The most red transition is found at 27624 cm^{-1}. By recording IR/R2PI spectra for the electronic ground state via the transitions of the R2PI spectrum as well as applying MATI spectroscopy (cf. Chapter 2.2), different isomers can be identified: By determination of the ionization potentials two isomers with electronic origins of 27624 and 27904 cm^{-1} can be assigned. However, the IR spectra in the spectral range of the hydroxyl and carbonyl stretching vibrations (3000 - 3800 cm^{-1} as well as 1500 - 1800 cm^{-1}) are identical, thus no direct structural discrimination is possible. Considering the results of *ab initio* und DFT calculations[73], the structures indicated in Figure 3.3a,b are by far the most stable, followed by the geometries depicted in Figure 3.3c,d. Each structure exhibits an

intramolecular hydrogen bond, for the isomers in Figure 3.3a,b this is formed between the hydroxyl group in position 2 to the C=O group of the carboxyl group whereas the isomers in Figure 3.3c,d form the hydrogen bond from the hydroxyl group in position 2 to the hydroxyl group of the carboxyl group. The structures depicted in Figure 3.3a,b (the same is valid for the geometries in Figure 3.3c,d) vary only in the relative orientation of the OH group in position 5, leading to identical calculated values for the OH and C=O stretching vibrations for isomers A and B (and for isomers C and D). The experimentally observed frequencies can unambigously be assigned to the isomers indicated in Figure 3.3a,b. In order to discriminate these two isomers, IR/R2PI spectra have been recorded in the upper fingerprint region (1100 - 1450 cm^{-1}). By extending the IR spectra to this range, both isomers can be assigned to their corresponding electronic origins in agreement with theoretical predictions.

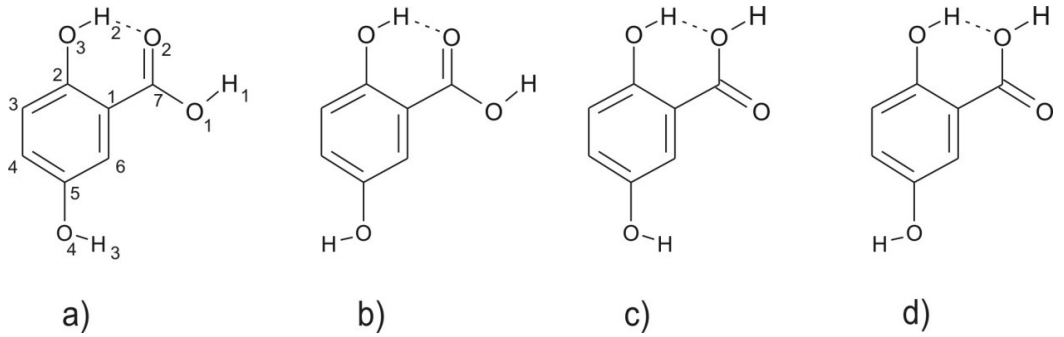

Figure 3.3: The four most stable isomers of DHB. The structures indicated a) and b) have been observed experimentally.

UV/IR/UV spectra (cf. Chapter 2.2.3) for the electronically excited state have been recorded in the range of 3000 - 3800 cm^{-1} for both isomers determined in the S_0 state. The spectrum exhibits two frequencies at 3603 and 3619 cm^{-1} for each isomer which are assigned to the OH stretching vibrations of the hydroxyl groups not involved in the hydrogen bond in agreement with theoretical predictions (TDDFT/B3LYP/TZVP)[73].

A possible proton transfer in the excited state should strongly influence the OH stretching vibration of the hydrogen bonded hydroxyl group as well as the C=O stretching vibration of the carboxyl group. The OH stretching vibration (of the intramolecular hydrogen bonded OH group) is strongly red shifted and probably broadened, so the analyses focused on the C=O stretching vibration. It turned out, that it is difficult to obtain

a reproducible UV/IR/UV spectrum (recorded via a depletion of the ion signal) for the electronically excited state in the range of 1450 - 1750 cm^{-1}. Instead an alternative technique has been applied, in which the energy of the ionizing laser is set 150 cm^{-1} below the ionization potential, and therefore only in the case of a resonant IR excitation the sum of both photons (IR+UV) is sufficient to ionize the molecule (cf. Chapter 2.2.3, Figure 2.5e and Figure 3.4). The advantage of this technique is that it is possible to measure against a zero base line. Thus the signal to noise ratio is excellent and even small effects can be observed.

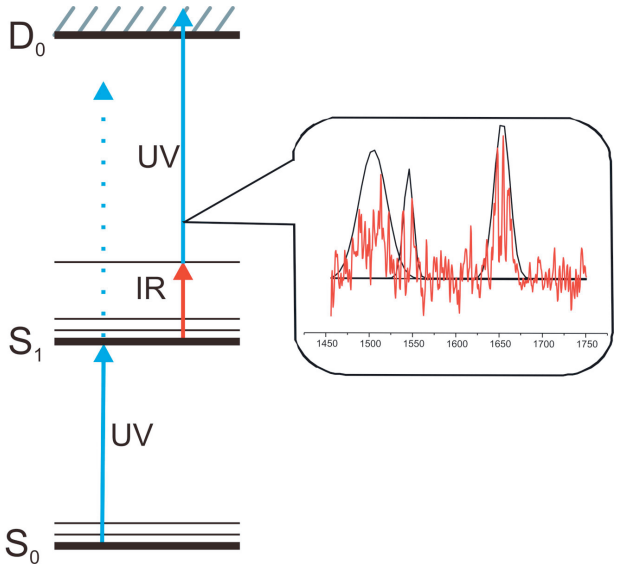

Figure 3.4: Scheme illustrating the UV+(IR+UV) technique for the electronically excited state

Experimentally three bands at 1508 cm^{-1}, 1552 cm^{-1} and 1655 cm^{-1} are observed with this technique for the most stable isomer in the S_0 state (Figure 3.3a). They fit ideally to the harmonically calculated vibrational frequencies (TDDFT/B3LYP/TZVP)[73] of the electronically excited state and can be assigned to coupled OH bending and C=O stretching vibrations. TDDFT calculations predict exactly one structure with an elongated OH bond for the S_1 state; no proton transfer including the formation of a second minimum is predicted[73]. This prediction is confirmed by the assignment of the experimentally obtained frequencies in the region of the C=O stretching vibrations.

The IR spectrum in the range of 1600 - 1800 cm^{-1} and 3200 - 3700 cm^{-1} for the D_0 state of the most stable isomer in the S_0 state (Figure 3.3a) has been recorded via IR/PIRI spectroscopy. The spectra exhibit three transitions at 3550 cm^{-1}, 3574 cm^{-1} and 1757 cm^{-1}. The former ones can be assigned to the OH stretching vibrations of the free hydroxyl

groups; the frequency of the hydrogen bonded OH group is - as in the S_1 state – shifted below the investigated spectral range. The transition at 1757 cm^{-1} is assigned to the C=O stretching vibration.

Hence DHB is a model system for the characterization of three electronic states (S_0, S_1, and the ionic ground state D_0) via the carbonyl stretching vibration. To attain this goal, appropriate methods are necessary: UV+(IR+UV) ionization has been applied for the first time to electronically excited states and the IR/PIRI spectrum has been recorded for the first time in the range of the carbonyl stretching vibrations. For further details see attached ref. [I].

3.2 3-Hydroxyflavone and 2-(2-Naphthyl)-3-hydroxychromone

Flavonoids represent a large group of organic natural dyes, being responsible for plant color. Flavonoids are known for their antioxidative and photoprotective effects[104], e.g. changes in the pathway of flavonoid synthesis occur upon UV-B radiation in plants.

Spectroscopically 3-hydroxyflavone (3-HF) (Figure 3.5) is of special interest as an excited state proton transfer (ESPT) takes place: After vertical excitation, a short lived excited state structure (S_1 state) is reached which relaxes on picoseconds timescale to the tautomeric form (S'_1 state). The ESPT of 3-HF was first observed by Kasha et al.[105] in 2-methylbutane solution. Investigations in various solvents as well as in matrices followed[106-120]. Especially the influence of the solvent on the ESPT time and the tautomer fluorescence lifetime as well as the influence of the temperature were analyzed. In solutions and in matrices the ESPT occurs on a femtosecond to picosecond timescale, in a molecular beam it is 2 ps[121].

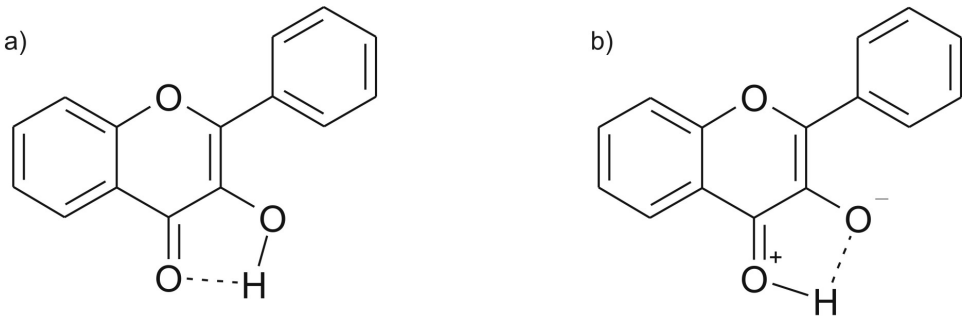

Figure 3.5: 3-Hydroxyflavone (3-HF) in its a) normal and b) tautomeric form.

Due to the pulse length of our laser systems a lifetime of the excited state on a nanosecond timescale is necessary for combined IR/UV experiments, as ionization occurs from thereon. The lifetime of the tautomeric structure differs from 890 ps in acetonitril[114] to 4 ns in methylcyclohexane[106, 116]. In an Ar matrix the lifetime of the tautomer fluorescence was determined to be 8.6 ns[111-113]. In the vapour phase the tautomer fluorescence lifetime is 1-2 ns[122] while in molecular beam experiments the lifetime of the tautomer was determined to be 14-15 ns[123], being sufficient for R2PI and combined IR/UV spectroscopy. Via fluorescence excitation spectroscopy in a supersonic jet the electronic origin was determined to be 28080 cm^{-1}[121, 123-125].

In order to obtain direct structural information, the IR spectra of the electronic ground state were recorded in the solid state[126], in solutions[126, 127], in an Ar matrix[128] and also in the gas phase[129, 130]. Up to now no detailed and direct structural information on the excited state was obtained.

A molecule that differs only in the second chromophore from 3-HF is 2-(2-naphthyl)-3-hydroxychromone (2-NHC) (Figure 3.6). The excited state proton transfer reaction was also observed for this molecule: In 3-methylpentane solution the tautomer fluorescence lifetime is about 5 ns depending on the temperature[131] whereas the ESPT occurs on a picoseconds timescale[132]. In molecular beam experiments the lifetime of the tautomer was determined to be 11-12 ns[123, 124], thus the molecule is suitable for the application of R2PI and combined IR/UV spectroscopy. The electronic origin was determined via fluorescence excitation spectroscopy to be 27291 cm^{-1} in a supersonic jet[123, 124].

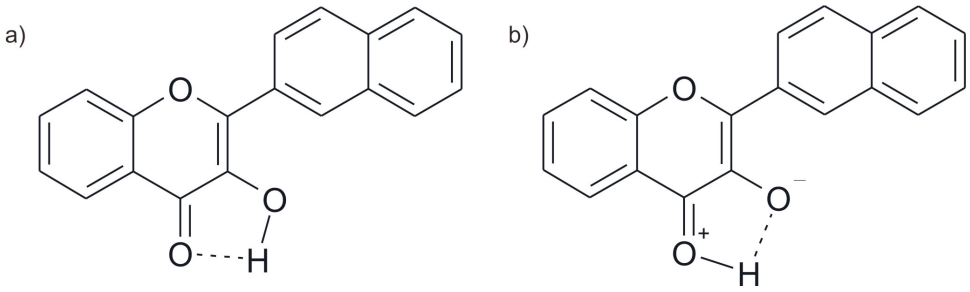

Figure 3.6: 2-(2-Naphthyl)-3-hydroxychromone (2-NHC) in its a) normal and b) tautomeric form.

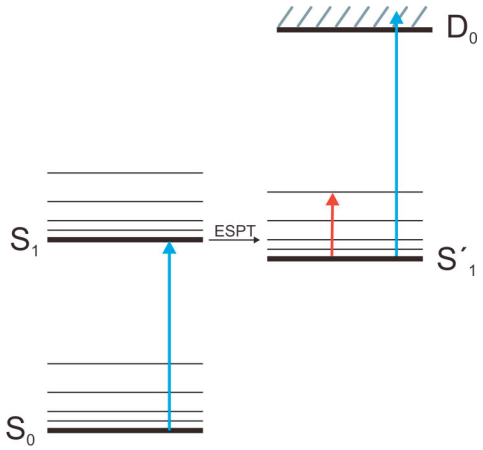

Figure 3.7: Schemes illustrating the IR/R2PI technique subsequent to an excited state proton transfer.

Up to now the ESPT process for both molecules was only analyzed via fluorescence spectroscopy, a detailed and direct structural investigation of the excited state tautomeric geometry via IR spectroscopy was not performed yet. UV/IR/UV spectroscopy offers the possibility to record spectra of electronically excited states[68, 69] (cf. Chapter 2.2.3), and in the cases of 3-HF and 2-NHC it has been successfully applied for the first time to an excited singlet state subsequent to an excited state proton transfer (cf. Chapter 2.2.3, Figure 2.5d and Figure 3.7).

3.2.1 Results for 3-HF and 2-NHC [II]

IR spectra for the electronic ground state of 3-HF have been recorded in the region of the OH stretching vibrations (2600 - 3800 cm^{-1}) and in the region of the C=O stretching vibrations (1450 - 1750 cm^{-1}). For a structural assignment, different geometries have been optimized and the calculated frequencies of the isomers[73] are compared to the experimentally obtained values. Harmonic calculations (TDDFT/B3LYP/TZVP)[73] predict the normal structure to be most stable in the electronic ground state while the tautomeric form is most stable in the electronically excited state (Figure 3.5). Based on the calculated frequencies in the region of the OH stretching vibrations as well as in the region of the C=O stretching vibrations, the normal form is assigned to the electronic ground state.

Experimentally the OH stretching vibration has been obtained at 3276 cm^{-1} in the electronic ground state and at 3350 cm^{-1} in the electronically excited state (carrier gas: neon). Scaled harmonic calculations (TDDFT/B3LYP/TZVP)[73] predict a strong red shift for the OH stretching vibration for the normal form, while it is blue shifted for the tautomeric form compared to the electronic ground state. Thus the proton transfer is verified, although both frequencies are calculated at higher energies (resulting from the unsatisfying description of the anharmonic potential energy curves of hydrogen bonded OH stretching vibrations by harmonic calculations). Anharmonic calculations along the reaction coordinate yield the assignment of an overtone rather than the fundamental[73].

The IR spectrum of 2-NHC has been recorded in the range of 3100 - 3460 cm^{-1} for the electronic ground and the electronically excited state. In analogy to 3-hydroxyflavone the

normal structure is unambiguously assigned to the electronic ground state, the tautomeric form to the electronically excited state (Figure 3.6).

The IR spectra of both molecules have been recorded in their electronic ground states and their electronically excited states. UV/IR/UV spectroscopy has been applied for the first time to an electronically excited state subsequent to an ESPT yielding detailed structural information about the reaction product after photoexcitation of 3-HF and 2-NHC. For further details see attached ref. [II].

3.3 3-HF$(H_2O)_n$ Clusters

Beside proton transfer reactions of photoexcited isolated molecules, the influence of solvent molecules is of interest in chemical and biological processes. By a gradual adding of solvent molecules, molecular beam experiments offer the possibility to investigate the isolated aggregate consisting of the molecule and its direct solvent environment. In the case of 3-HF the question of the influence of water aggregation on the ESPT is discussed controversially: The electronic origins of the mono- as well as of the dihydrate of 3-hydroxyflavone were determined to be 27772 cm^{-1} and 27470 cm^{-1} respectively[123, 124]. Both water clusters show no tautomer fluorescence excited at their origins. Thus, the ESPT is circumvented by adding water molecules. The same results were obtained in an Ar matrix concerning the dihydrate, whereas the monohydrate exhibits tautomer fluorescence at 490 - 575 nm[113]. In superfluid helium droplets, the ESPT was confirmed for 3-HF as well as for its aggregates with one and two water molecules[133].

Furthermore, the influence of methanol on the ESPT of 3-HF was investigated in a supersonic jet[134] as well as in an Ar matrix[135]. The results correspond to those of the water complexes: The tautomer fluorescence was observed in the matrix excited at 365 nm whereas no ESPT was found in a molecular beam with a similar excitation wavelength of 366 nm. As all investigations focused on fluorescence measurements, no direct structural information about the electronic ground or the electronically excited state were obtained.

Another interesting aspect is, that the hydrates of 3-HF are model systems for a proton or hydrogen transfer along a solvent wire as water molecules can be inserted between the hydroxyl and the carbonyl group. 7-Hydroxyquinolin was analyzed in a supersonic jet with respect to solvent wire reactions[21-35]: The transfer starts at the hydroxyl group along the solvent molecules to the accepting nitrogen atom. Methanol[21], ammonia[22, 24, 26-34] and water molecules[23, 25, 32, 35] served as solvents. In the case of the aggregates with methanol molecules, wires are formed by two and three solvent molecules. However the proton/hydrogen transfer occurs only for 7-hydroxyquinolin$(CH_3OH)_3$[21].

A minimum of two solvent molecules is also needed in the case of ammonia to bridge the donating and accepting group; for more than four ammonia molecules additional topologies occur[26]. The proton/hydrogen transfer after vertical excitation via the origin was assigned to the aggregates with a minimum of four ammonia molecules[22, 24, 26-28].

However the proton/hydrogen transfer in the excited state can be induced for the cluster with three ammonia molecules by exciting low frequency ammonia wire vibrations[29-34].

Changing the solvent molecule to water or even the introduction of one single water molecule stops the proton/hydrogen transfer as the energy barrier is increased[23, 25, 32, 35]. In a mixed wire in which the first location is occupied by an ammonia molecule, the first transfer (7-hydroxyquinoline to ammonia) takes place[32, 35].

7-Azaindole was analyzed with respect to solvent wire reactions as well[36-40]: Methanol[36-38] and water[39, 40] served as solvent molecules. In the case of methanol, a transfer was observed from the NH group to the accepting nitrogen atom for aggregates with two solvent molecules excited at their origin[37, 38]. In analogy to 7-hydroxyquinoline, no proton transfer has been observed for water as a solvent[39, 40].

All information on the solvent wire of 7-hydroxyquinoline and 7-azaindole mainly result from fluorescence, UV- and UV/UV double resonance techniques (IR spectroscopy has only been applied to 7-azaindole in the electronic ground state[36]). Thus no structural assignments for the excited state were obtained. In this work the IR spectra of the electronic ground state of the mono- and the dihydrate as well as the IR spectra of the electronically excited states of the aggregate with two water molecules are presented. In combination with *ab initio* and (TD)DFT calculations[73] a structural assignment to all states is possible. Thus the question whether an ESPT occurs for the aggregates with water which has not been observed for 7-hydroxyquinoline and 7-azaindole can be clarified. Furthermore the arrangement of the water molecules in the aggregates is determined.

3.3.1 Results for 3-HF(H_2O)$_1$ [III]

The monohydrate is formed less prominently than the dihydrate. Thus only the IR spectrum of the electronic ground state can be recorded in the range of 2700 - 3800 cm^{-1} and in the range of 1450 - 1750 cm^{-1}.

For the aggregate with one water molecule different binding motives, whose structures and frequencies have been calculated at the DFT/B3LYP/TZVP level[73], are feasible. The experimentally obtained spectrum can be explained by an overlay of the two most stable

isomers: The structure in which the water molecule is inserted between both functional groups and a geometry in which the water molecule is hydrogen bonded to the carbonyl group have been assigned to the electronic ground state (Figure 3.8).

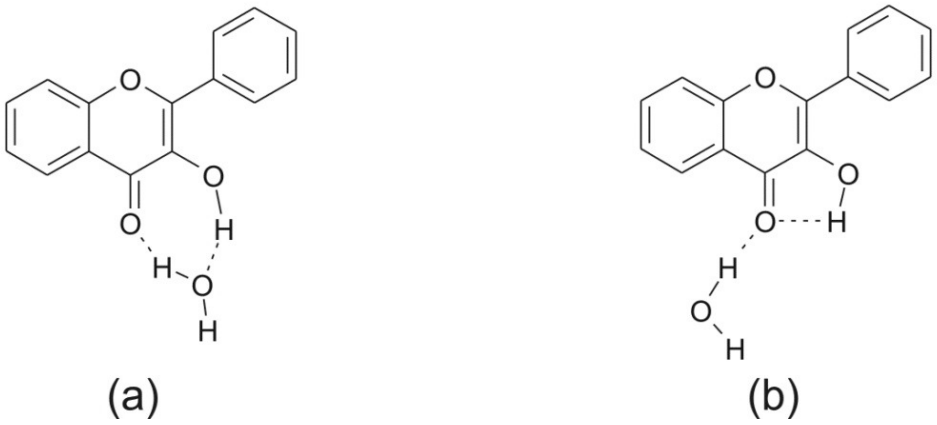

Figure 3.8: Assigned structures to the electronic ground state of 3-HF$(H_2O)_1$: (a) inserted structure and (b) structure in which the water molecule is bonded to the carbonyl group.

3.3.2 Results for 3-HF$(H_2O)_2$ [III]

The IR spectrum of the prominently formed dihydrate has been recorded in the range of 2700 - 3800 cm^{-1} as well as in the range of 1150 - 1750 cm^{-1}. Based on harmonic calculations (DFT/B3LYP/TZVP) of various geometries including normal and proton transferred structures[73], the spectrum can be assigned to an overlay of the two most stable isomers (Figure 3.9): A structure in which both water molecules are inserted between the functional groups (isomer *I*, Figure 3.9a) and a geometry in which one water molecule is inserted while the second one is hydrogen bonded to the first one (isomer *D*, Figure 3.9b). Both species are overlaid in a broad electronic transition; therefore the IR spectra of the two isomers cannot be separated by the choice of the UV excitation wavelength: The IR spectrum recorded via several excitation energies - including both, maxima and minima of the R2PI spectrum - turn out to be identical for all chosen wavelength.

In the case of the electronically excited state the IR spectrum has been recorded in the range of 2700 - 3800 cm^{-1}. The question whether a proton transfer occurs subsequent to

photoexcitation is of special interest. Based on the fact that two isomers are assigned to the electronic ground state, these structures as well as their tautomeric forms have been calculated for the excited state (TDDFT/B3LYP/TZVP)[73]. The proton transferred species turn out to be most stable. By comparing the experimentally obtained spectrum to the calculated frequencies, structure *D* can unambiguously be assigned to the excited state. Furthermore the same overlay as in the electronic ground state (isomer *D* and *I*) is most probable. Anyway the UV/IR/UV spectrum recorded via an excitation with a low excess energy (28080 cm^{-1}) yields no evidence for a proton transfer.

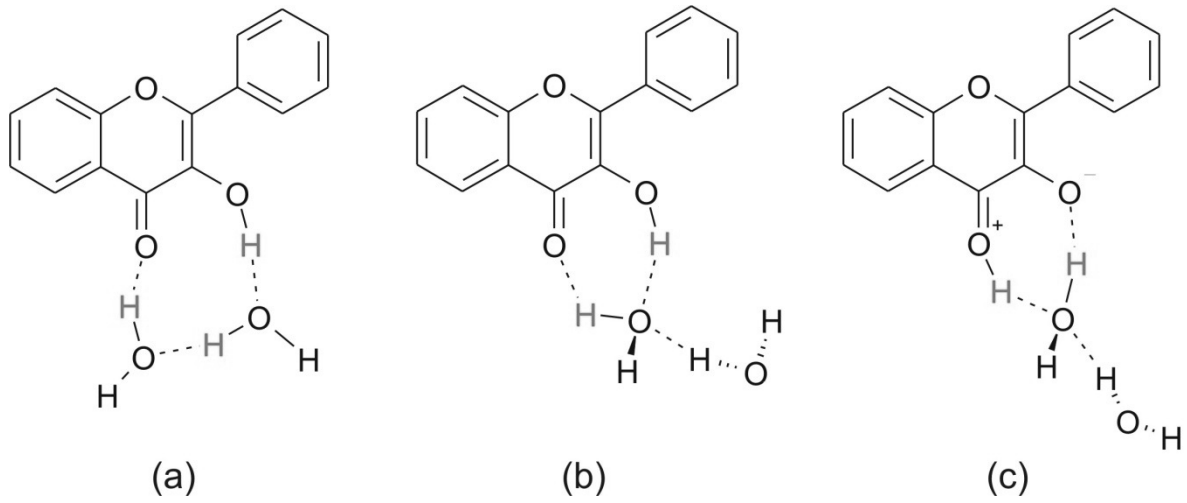

Figure 3.9: Structures of 3-HF(H_2O)$_2$: (a) inserted structure *I* (b) structure *D*, in which the second water molecule is hydrogen bonded to the first one (c) proton transferred structure *DT*.

By raising the UV excess energy by yet another 500 cm^{-1} compared to excitation at 28080 cm^{-1} (overall excess energy: ~900 cm^{-1}), the UV/IR/UV spectra exhibit further transitions which are in good agreement with the calculated frequencies of the *DT*-structure (Figure 3.9c). Thus a proton transfer along a solvent wire can be induced by exceeding an energy barrier, leading to the more stable tautomeric structure.

UV/IR/UV spectroscopy has been applied to the electronically excited states of the dihydrate of 3-HF, yielding information on structural changes due to a cooperative proton transfer along a water molecule: By increasing the UV excitation energy, i.e. the excess energy in the electronically excited state, a proton transfer along a proton wire can be induced. The product has been analyzed by IR spectroscopy again, indicating the formation of the isomer *DT*. Therefore 3-HF(H_2O)$_2$ represents the first isolated proton wire

investigated by combined IR/UV spectroscopy in the excited state, yielding unambiguous structural information. Furthermore so far unknown geometries can be identified in the electronic ground state as well as in the electronically excited states by applying combined IR/UV spectroscopy. For further details see attached ref. [III].

3.4 Xanthone

Derivatives of xanthone occur as plant pigments in exotic fruits such as the mangosteen fruit. They are used as additives in the polymerization of polyester in order to provide resistance to degradation by UV light. Furthermore some derivatives show antioxidative effects.

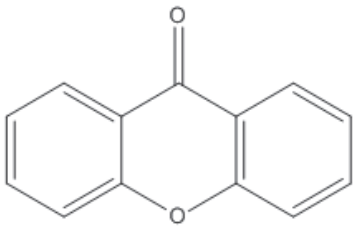

Figure 3.10: Xanthone.

Xanthone (Figure 3.10) was analyzed via phosphorescence, fluorescence and transient absorption spectroscopy with regard to the energy, the lifetime and the character of its electronically excited states. Most of these investigations were carried out in solutions, focusing on the influence of the solvent and the temperature dependence[136-152].

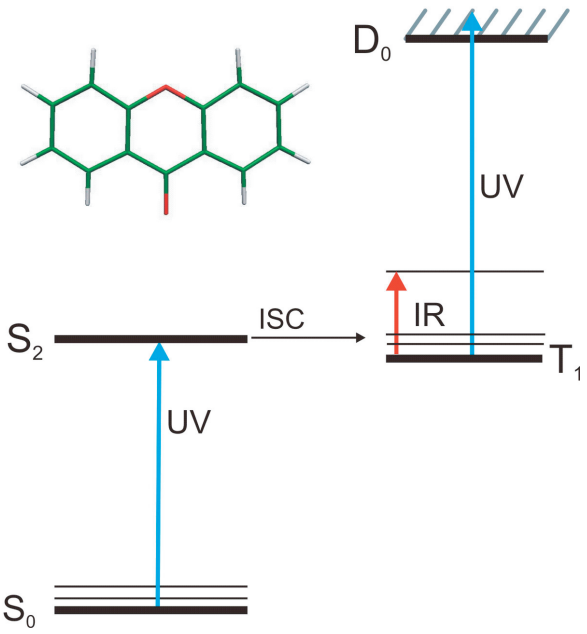

Figure 3.11: Scheme illustrating the IR/R2PI technique subsequent to an *Intersytem Crossing*.

Xanthone was also investigated via phosphorescence and fluorescence spectroscopy in a supersonic jet[153, 154]: The origins of the S_1 ($n\pi^*$), the S_2 ($\pi\pi^*$) and the T_1 ($n\pi^*$) state were determined to be 26939 cm^{-1}, 30718 cm^{-1} and 25808 cm^{-1} respectively. The phosphorescence of the T_1 state was observed in a molecular beam after excitation to the S_2 state, thus the S_2 state couples directly with the T_1 state, leading to an efficient *Intersystem Crossing (ISC)* in accordance to El-Sayed´s rule[155], predicting efficient *ISC* between a $\pi\pi^*$ and a $n\pi^*$ state.

In order to apply UV/IR/UV spectroscopy for the first time to triplet states without a messenger molecule, xanthone (Figure 3.10) was chosen as an archetype molecule due to its efficient *ISC*, with the intention to investigate a triplet state subsequent to an *ISC* (cf. Chapter 2.2.3, Figure 2.5d and Figure 3.11).

3.4.1 Results for Xanthone [IV]

In this work two-color R2PI spectra have been recorded in the range of the $S_1 \leftarrow S_0$, the $S_2 \leftarrow S_0$ as well as the $T_1 \leftarrow S_0$ transition. The ionizing laser has been set to 44053 cm^{-1} in order to exceed the ionization potential (69686 cm^{-1} (8.64 eV)[156] and 68718 cm^{-1} (8.52 eV)[157]) even if ionization originates from the T_1 state. No ion signal has been obtained in the region of the $S_1 \leftarrow S_0$ transition and direct triplet excitation has not been successful. In the range of the $S_2 \leftarrow S_0$ excitation three bands have been obtained with the origin at 30729 cm^{-1}. The additional transitions at 218 cm^{-1} and 249 cm^{-1} are assigned to low frequency vibrations of the S_2 state. The ion current (excitation laser fixed at 30729 cm^{-1}) yields a maximum ion signal at 43478 cm^{-1}, clearly indicating that ionization originates from the T_1 state.

The IR/R2PI spectrum for the electronic ground state has been recorded in the range of 1250 - 1750 cm^{-1}. The calculated frequencies (DFT/B3LYP/TZVP)[73] fit excellently to the experimentally obtained values and the transition at 1692 cm^{-1} is assigned to the C=O stretching vibration whereas the other bands are assigned to combined CC stretching and CH bending modes.

For the T_1 state the IR/R2PI spectrum has been recorded in the range of 1250 - 1750 cm^{-1}. Again, the calculated frequencies of the T_1 state (DFT/B3LYP/TZVP)[73] match the experimentally obtained frequencies excellently: The transitions are assigned to combined CC stretching (ring deformation vibrations) and CH bending modes.

The IR spectra of the S_0 as well as the T_1 state of xanthone have been recorded by combined IR/UV spectroscopy and the obtained transitions have been assigned in combination with DFT calculations. UV/IR/UV spectroscopy has been applied to triplet states subsequent to an *ISC* and without using messenger molecules for the first time. For further details see attached ref. [IV].

3.5 Caged Compounds

Caged compounds are molecules with a photolabile protective group that release active components after electronic excitation[41]. For this *o*-nitrobenzyl groups are commonly used, however other components like *p*-nitrophenyl-, phenacyl- or 4-methylcoumarin compounds are also suitable as protective groups (cf. example [158-163]). The release of the active component can be used to insert it into cells: For example cyclic adenosine monophosphate (cAMP) was bonded to an *o*-nitrobenzylic protective group. Thus the molecule is hydrophobic and can diffuse into a cell. There it can be released by a laser pulse[42, 43]. The same technique was applied to adenosine triphosphate[41].

Requirements for caged compounds are hydrophilic properties, stability concerning hydrolysis, low activation energy for the photochemical reaction and the property of being inert to biological systems. Furthermore the photochemical release is required to be fast, the quantum yield high and their coproducts should have no side effects.

Several spectroscopic analyses in solutions or in matrices gave evidence, that *o*-nitrobenzylic derivatives follow this reaction scheme subsequent to photoexcitation[158-160]:

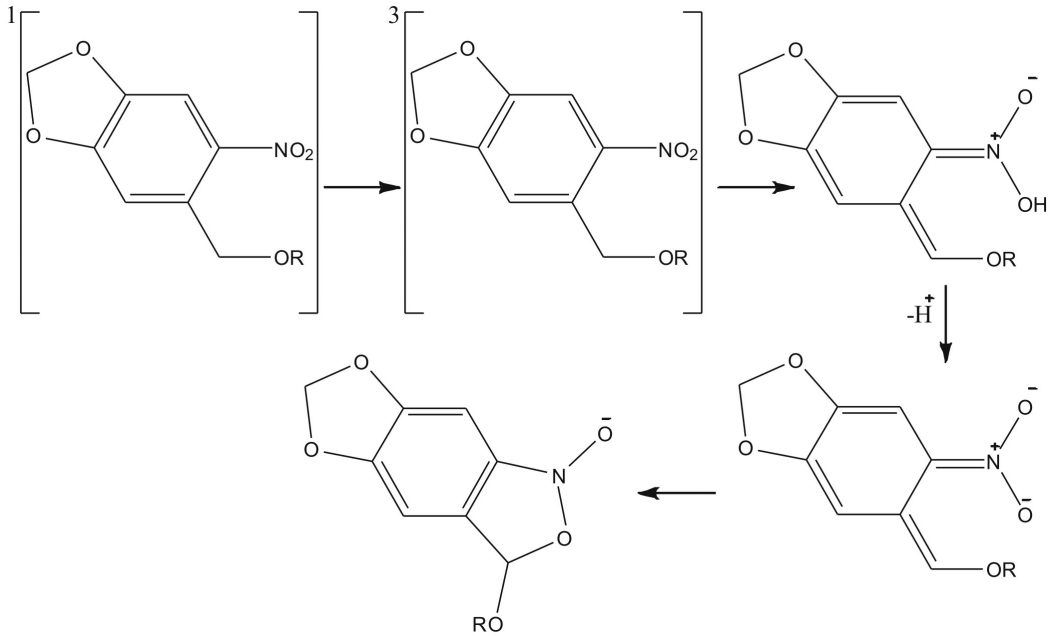

Figure 3.12: Proposed reaction scheme for *o*-nitrobenzylic derivatives subsequent to photoexcitation. Herein compounds with R=H and R=Ac have been examined.

After photochemical excitation via an UV photon, *Intersytem Crossing (ISC)* to a triplet state occurs. Then a proton is transferred, forming an aci-nitro compound. By adding a base deprotonation occurs, followed by cyclisation.

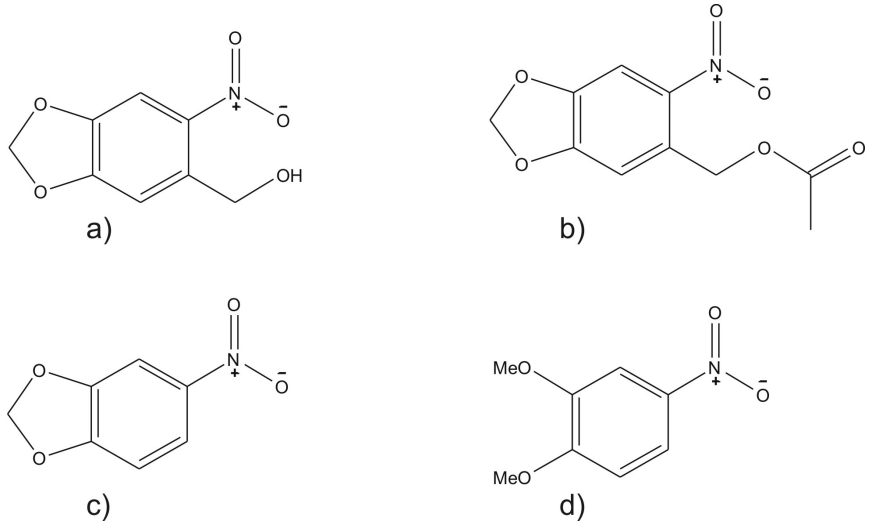

Figure 3.13: Caged compounds based on nitrobenzenes:

a) 6-Nitropiperonylalcohol

b) 6-Nitropiperonylacetate

Model substances without a reactive group in *o*-position:

c) 3,4-Methylendioxynitrobenzene

d) 3,4-Dimethoxynitrobenzene.

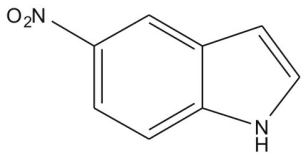

Figure 3.14: 5-Nitroindole.

In this work *o*-nitrobenzylic derivatives containing a hydroxyl group (Figure 3.13a) as well as compounds containing an acetyl group (Figure 3.13b) have been investigated. Besides these caged compounds 3,4-methylendioxynitrobenzene (Figure 3.13c) and 3,4-dimethoxy-nitrobenzene (Figure 3.13d) have been analyzed as precursor molecules. The investigation of these two molecules focused on the effect of the two methoxy groups instead of the

dioxolane substituent onto the stability of the nitro aromatic compound after electronic excitation. Additionally the influence of a second aromatic compound in *meta* and *para* position onto the photostability has been investigated by analyzing 5-nitroindole (Figure 3.14).

In order to obtain structural information about the electronic ground states as well as the electronically excited states, combined IR/UV spectroscopy has been applied to these molecules. The major problem of these substances is their reactivity after electronic excitation, resulting in fragmentation, which should be dependent on the excitation wavelength. Additionally fragmentation can also occur in the ionic state. Due to the fact that the resulting ions of the R2PI process have been analyzed in a time-of-flight mass spectrometer, fragmentation pathways can be observed and thus information about the reaction coordinate are obtained.

3.5.1 Results for 6-Nitropiperonylalcohol

The gas phase absorption spectrum (T = 122 °C) of 6-nitropiperonylalcohol (Figure 3.15) exhibits three transitions with maxima at 222 nm (I), 278 nm (II) as well as 306 nm (III). The first two bands (I and II) can be assigned qualitatively to ππ* charge-transfer transitions between the aryl group and the nitro group. In the case of transition (I) an additional contribution from an excitation of the π-system (without the nitro group) to Rydberg states is postulated. The most bathochrome band (III) is characterized by a ππ* charge-transfer between the aryl group with participation of the oxygen atoms to the nitro group[164].

One-color and two-color R2PI spectra have been recorded in the range of the electronic resonances (I) to (III) aiming to obtain a parent ion of the 6-nitropiperonylalcohol (m/z = 197). In all measurements - including various wavelengths for the ionizing laser - no parent ion has been detected. Exemplarily two mass spectra which resulted for wavelengths of 230 nm and 299 nm are depicted in Figure 3.16. Furthermore by setting the ionizing laser to another wavelength (two-color ionization) only an overlay of the mass spectra recorded with one-color conditions - and therefore no parent ion at 197 Da - is observed. It is

noteworthy, that in the case of the shorter wavelength of 230 nm (excitation in the range of transition (I)) fragments of higher masses are preferred.

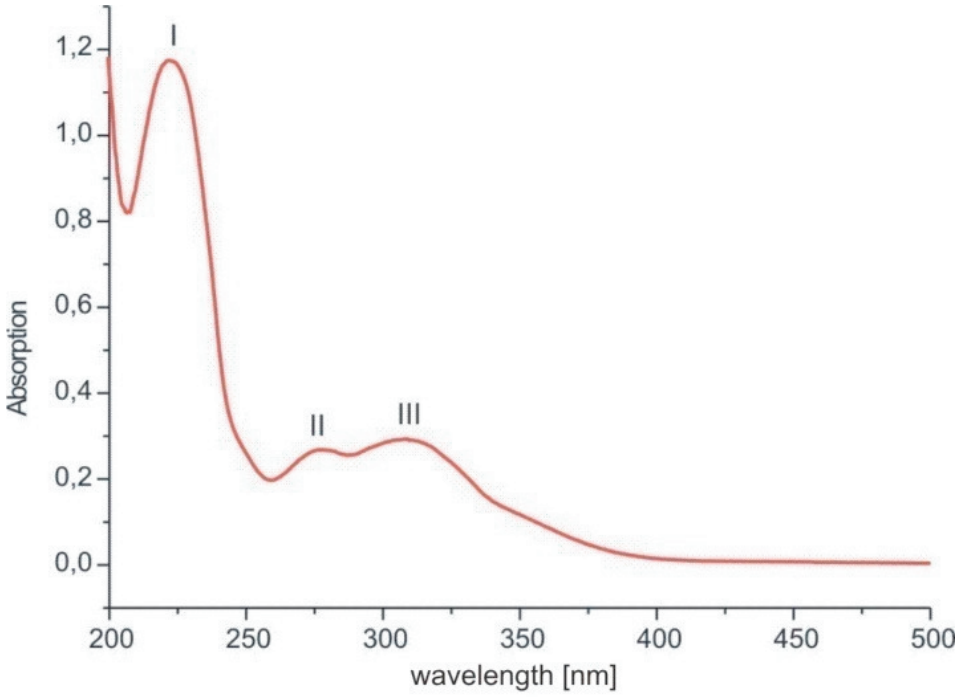

Figure 3.15: Gas phase UV absorption spectrum of 6-nitropiperonylalcohol (T = 122 °C).

The obtained fragment of 180 Da is explained by the loss of the alcoholic hydroxyl group. Depending on the excitation wavelength, most prominent fragments are obtained at 137 Da and 167 Da. The mass signal at 167 Da results from a rearrangement to a nitrite followed by the release of the NO group (Figure 3.17). This mechanism was discussed in several publications for different nitroalkanes or nitroaromatics (*o*-nitrotoloul) (cf. example [165-168]). Additionally these publications proposed a mechanism in which NO_2 is released and fragments further to NO and O. For this reaction a fragment of 151 Da should be detected instead of - or additionally to - the fragment of 167 Da.

The mass signal at 137 Da results from the loss of the NO group plus the side chain in *o*-position (release of formaldehyde) (Figure 3.24). The analogue mechanism in which the side chain is released, is observed for 6-nitropiperonylacetate (cf. Chapter 3.5.2 and Figure 3.24).

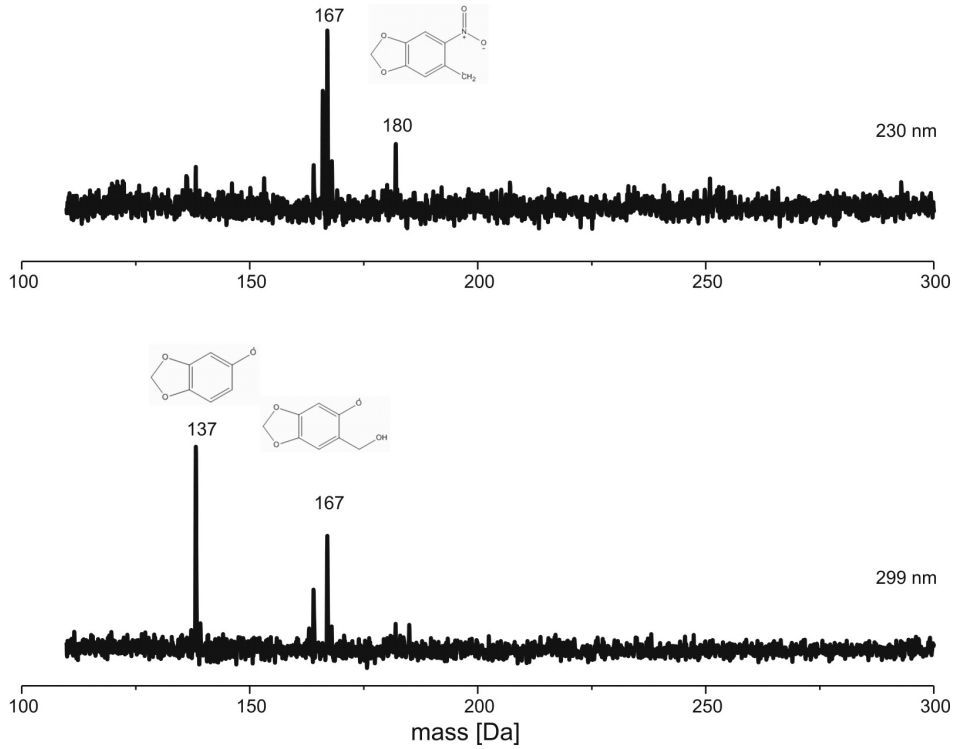

Figure 3.16: Fragmentation pattern of 6-nitropiperonylalcohol at different excitation energies.

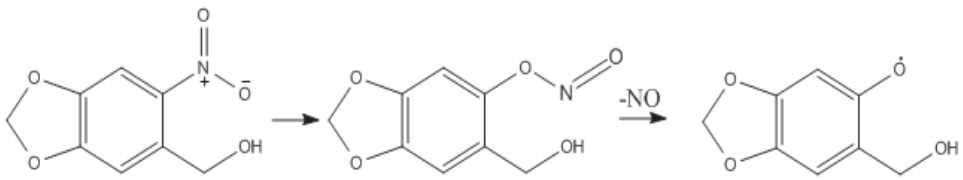

Figure 3.17: Reaction scheme for the fragmentation in the excited state.

R2PI spectra with sharp transitions have been recorded via the mass traces of 137 Da and 167 Da. The corresponding spectra are illustrated in Figure 3.18 and 3.19, the first one has been recorded by one-color R2PI, the second one by two-color R2PI (the corresponding spectrum using one-color R2PI exhibits the same transitions). It should be noted, that the fragment of 167 Da shows no R2PI signals in the range of the spectrum of mass 137 Da (Figure 3.18, 31100 - 31440 cm^{-1}) and vice versa.

R2PI spectra are important for the characterization of the obtained species and conclusions about the reaction mechanism are possible, particularly with regard to reaction processes in other caged compounds as 6-nitropiperonylacetate (cf. Chapter 3.5.2).

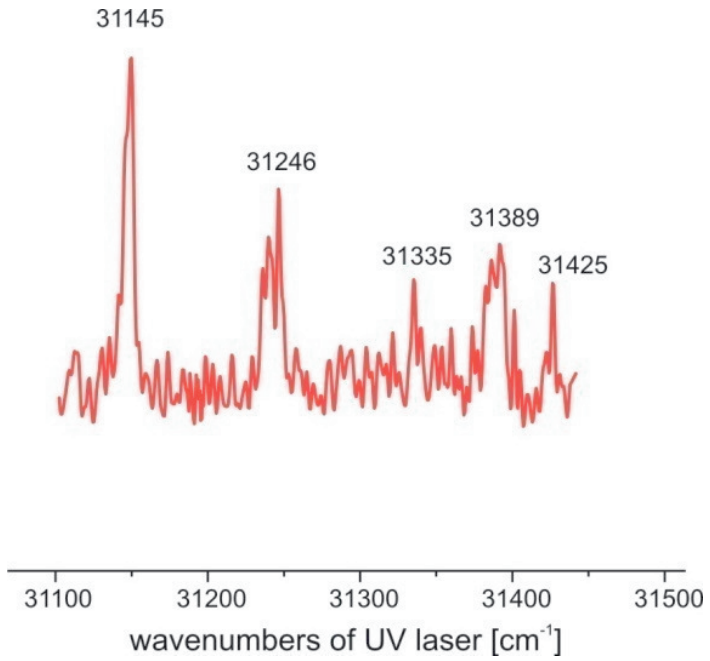

Figure 3.18: R2PI spectrum recorded via the mass trace of the fragment of 137 Da.

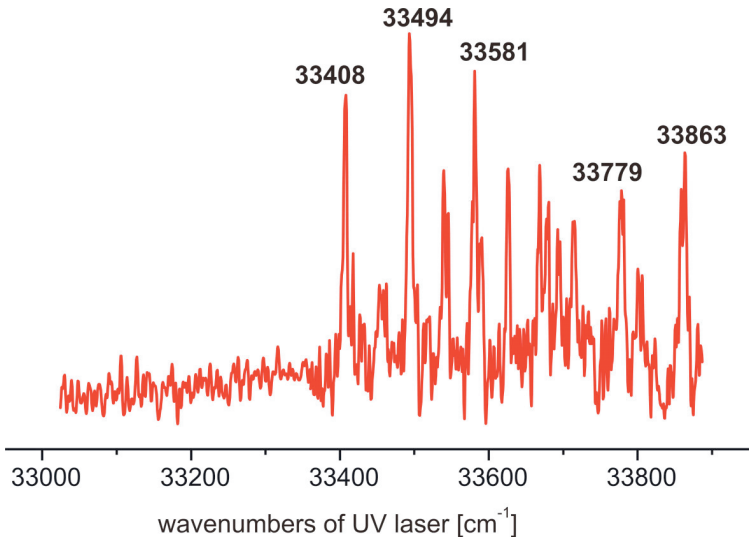

Figure 3.19: Two-color R2PI spectrum recorded via the mass trace of the fragment of 167 Da (ionizing laser: 230 nm).

As pointed out in Chapter 2.2.3, combined IR/UV spectroscopy can be applied to electronic ground states as well as to electronically excited states. In the case of the electronic ground state, the IR photon arrives prior to the UV photons, thus it is negligible whether fragmentation occurs after electronic excitation: The IR photon excites vibrations

of the intact molecule. Nevertheless it is necessary that the depletion effect is detectable even after fragmentation in the excited state in order to apply the IR/R2PI technique.

The IR/R2PI spectrum (Figure 3.20) in the range of 3520 - 3760 cm^{-1} recorded for the electronic ground state via the mass trace of 167 Da (excitation laser: 33494 cm^{-1} and ionizing laser: 230 nm) exhibits a band at 3592 cm^{-1}. This transition is assigned to the OH stretching vibration of the neutral, undecomposed molecule.

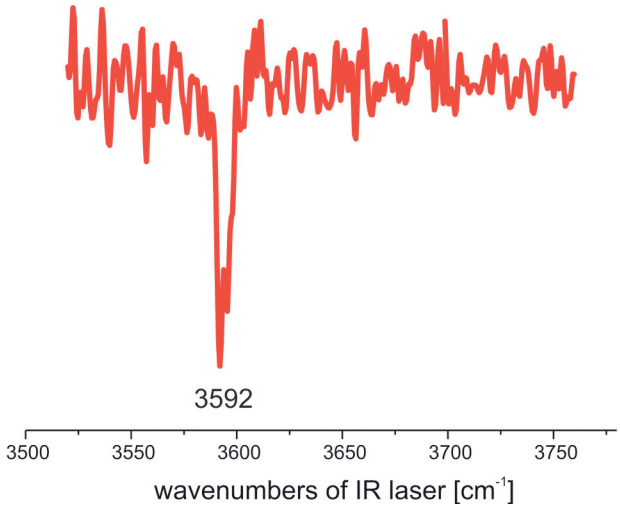

Figure 3.20: IR/R2PI spectrum of the electronic ground state recorded via the mass trace of the fragment of 167 Da.

A similar molecule that was also analyzed in molecular beam experiments is benzyl alcohol[169]. As the investigated 6-nitropiperonylalcohol it possesses a CH_2OH group bonded to an aromatic compound. Two isomers were assigned in the supersonic jet: A structure which is completely in-plane and a structure in which the OH group is out-of-plane interacting with the π-electrons of the benzyl ring (Figure 3.21). The experimentally obtained frequencies are 3650 cm^{-1} and 3587 cm^{-1}, respectively[169]. The observed frequency for the 6-nitropiperonylalcohol at 3592 cm^{-1} offers a good agreement to the frequency of the OH stretching vibration of the gauche-type structure. Therefore a similar interaction with the aromatic system could be existent for the caged compound. Anyhow it should be noted that the hydroxyl group can be hydrogen bonded to the oxygen atom of the nitro group, leading to an additional red shift of the vibrational frequency.

Figure 3.21: Confomers of benzyl alcohol, all in-plane structure (left side) and the gauche-type conformer (right side)[169].

The IR spectra of the excited state of 6-nitropiperonylalcohol are of special interest, but these could not be recorded successfully via the mass traces of the fragments.

3.5.2 Results for 6-Nitropiperonylacetate

As no parent ion has been obtained for 6-nitropiperonylalcohol, the alcohol has been esterified in order to increase the stability of the molecule after electronic excitation. The obtained 6-nitropiperonylacetate (m/z = 239) (Figure 3.13b) has been investigated by one-color and two-color R2PI spectroscopy in the same spectral range as the alcohol. Unfortunately no parent ion has been detected either. By comparing the mass spectra of the acetate (Figure 3.22) to the ones of the alcohol, it can be seen that one fragment of the same mass appears, additionally other fragments result from identical fragmentations: The loss of the NO group (fragment mass 209 Da) or the CH_3-OCO group (fragment mass 180 Da, in analogy to releasing the hydroxyl group in the case of the alcohol) and the loss of both, the NO group and the side chain in *o*-position (fragment mass 137 Da). Ion signals for masses which are higher than the parent ion (m/z = 239) can either be due to aggregation of fragments or to small impurities of the substance (resulting from synthesis) which are easy to ionize.

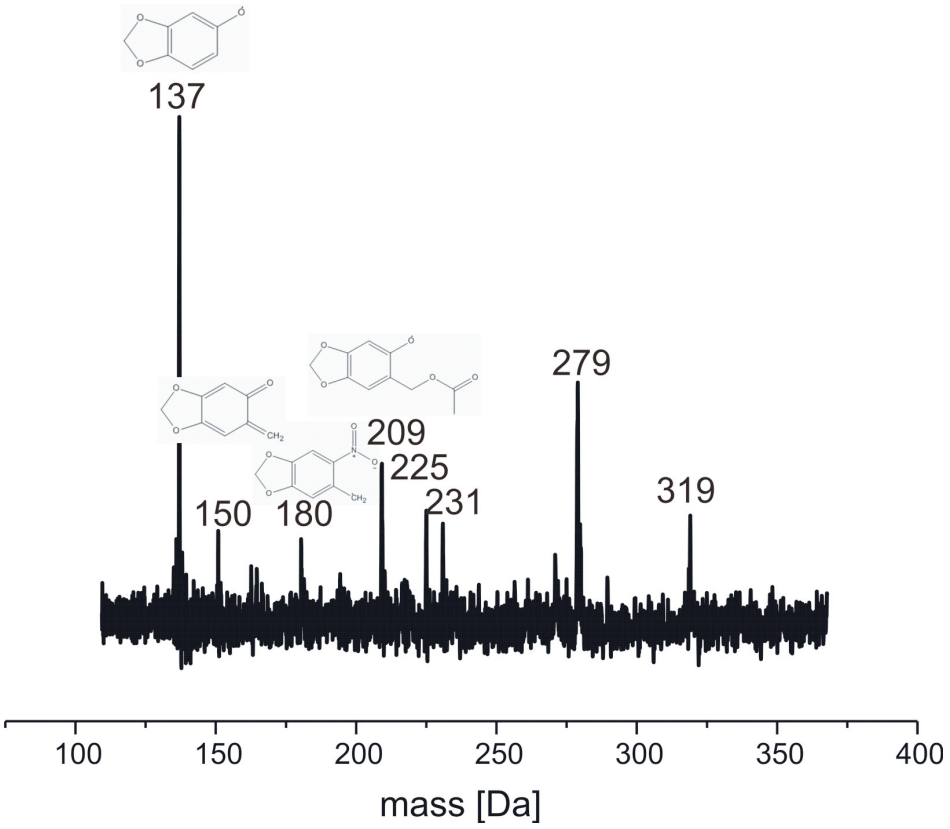

Figure 3.22: Fragmentation pattern of 6-nitropiperonylacetate (excitation laser: 33670 cm^{-1} and ionizing laser: 40000 cm^{-1}).

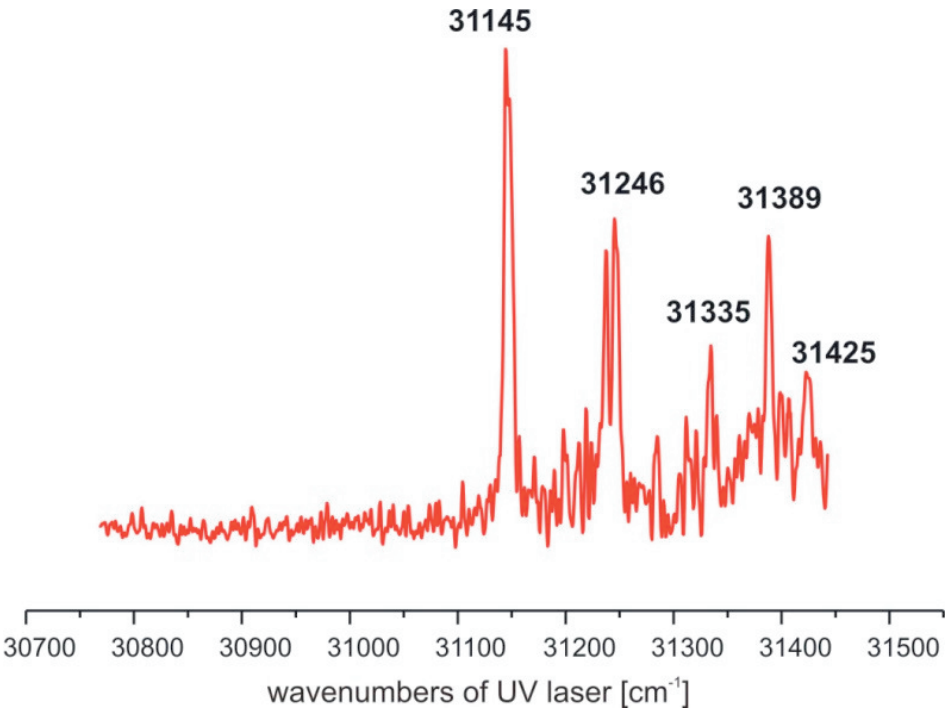

Figure 3.23: R2PI spectrum recorded via the mass trace of the fragment of 137 Da.

In order to characterize the fragments, R2PI spectra have been recorded. The one-color R2PI spectrum (Figure 3.23) recorded in the range of 30770 - 31440 cm^{-1} exhibits sharp resonances for the fragment of 137 Da. The same spectrum was obtained for the two-color process. The experimental transitions are identical to the ones obtained for the same fragment in the case of the alcohol (Figure 3.18). Thus the same species is formed in both cases. This is a clear indication for analogue fragmentation mechanisms, in which an intramolecular rearrangement leads to the nitrite, followed by releasing the NO group and the side chain in *o*-position (Figure 3.24).

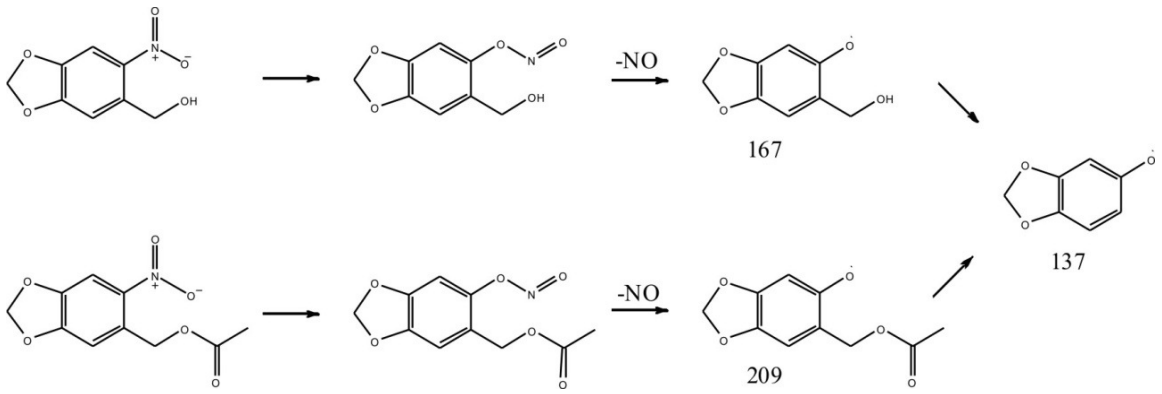

Figure 3.24: Reaction scheme for the loss of NO plus the sidechain in *o*-position leading to a fragment of 137 Da for 6-nitropiperonylalcohol (upper trace) and 6-nitropiperonylacetate (lower trace).

3.5.3 Results for 3,4-Methylendioxynitrobenzene

As no parent ion has been detected for the caged compounds, the skeletal structure of the nitro compounds without a side chain in *o*-position to the nitro group has been analyzed. This offers the possibility to investigate the stabilization obtained by different substituents in *meta* and *para* position to the nitro group. In contrast to the caged compounds, a parent ion has been obtained in the case of 3,4-methylendioxynitrobenzene (Figure 3.13c) even by a one-color R2PI process (Figure 3.25). The parent ion (m/z = 167) is the most dominant mass signal for an excitation wavelength of 230 nm, whereas strong fragmentation occurs for an excitation wavelength of 270 nm. This result is in agreement to the analyses of the caged compounds, i.e. via excitation of the first absorption band

(Figure 3.15) fragments of higher masses are preferred. In the case of 3,4-methylendioxynitrobenzene it can almost be suppressed completely (Figure 3.25). The fragment of 121 Da (most dominant signal for the longer excitation wavelength) results from releasing NO_2, the fragment of 137 Da results from the loss of NO (cf. Chapter 3.5.1 and 3.5.2).

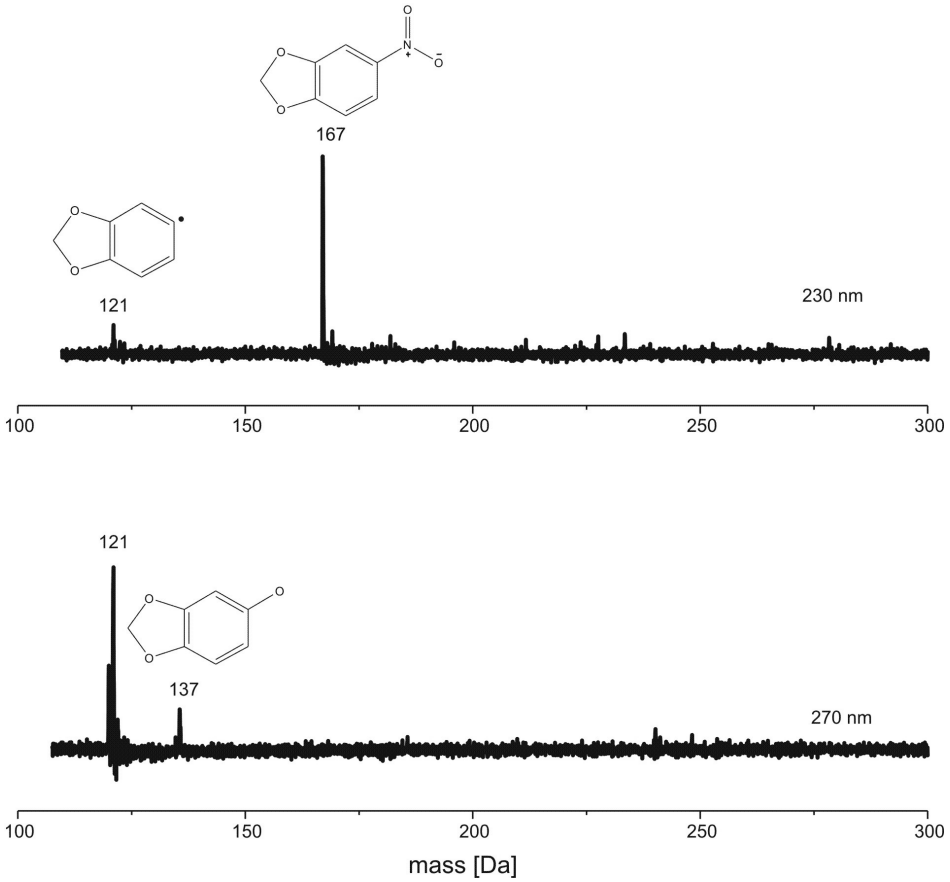

Figure 3.25: Fragmentation pattern of 3,4-methylendioxynitrobenzene at different excitation energies.

The R2PI spectra for 3,4-methylendioxynitrobenzene in the range of the electronic transitions (I) and (II) are shown in Figure 3.26. No sharp resonances have been obtained; the spectra exhibit only broad transitions.

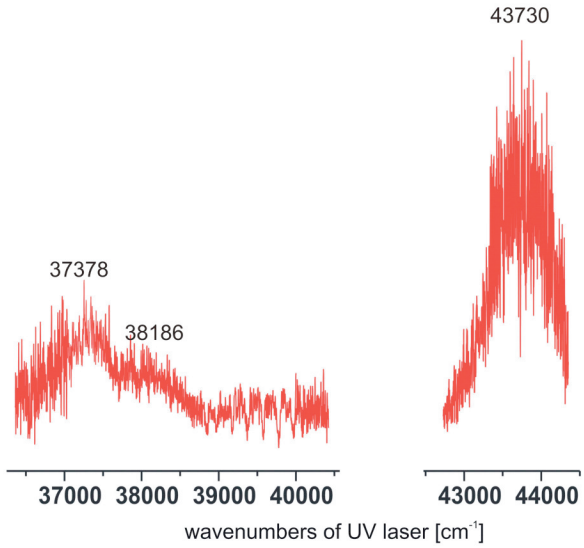

Figure 3.26: R2PI spectrum of 3,4-methylendioxynitrobenzene.

3.5.4 Results for 3,4-Dimethoxynitrobenzene

Furthermore 3,4-dimethoxynitrobenzene (Figure 3.13d) has been investigated. The interest is focused on the influence of the substitution of the dioxolane group by two methoxy groups onto the stability of the nitro aromatic compound after electronic excitation. For this molecule the parent ion has been obtained as well, and as in the case of 3,2-methylendioxynitrobenzene it is only formed by the shorter excitation wavelength of 230 nm (Figure 3.27). This behavior is in agreement to the results for all the investigated species concerning the formation of parent ions or - in the case of the caged compounds - the formation of larger fragments subsequent to excitation via the electronic transition (I).

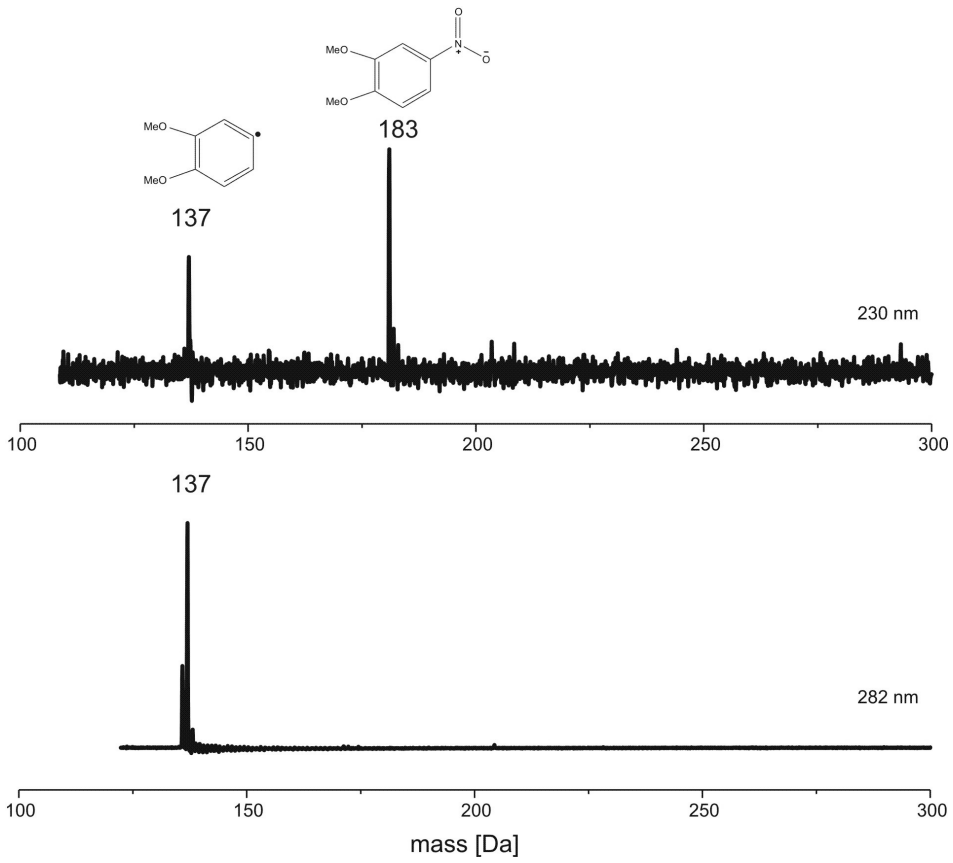

Figure 3.27: Fragmentation pattern of 3,4-dimethoxynitrobenzene at different excitation energies.

As for 3,4-methylendioxynitrobenzene (Figure 3.25) the mass spectrum exhibits an additional fragment (m/z = 137) resulting from the loss of NO_2. With respect to the obtained parent ions, the formation of this fragment is suppressed more efficiently for 3,4-methylendioxynitrobenzene compared to 3,4-dimethoxynitrobenzene. Thus it can be concluded, that the dioxolane substituent increases the stability of the nitro aromatic compounds after electronic excitation.

3.5.5 Results for 5-Nitroindole

The previous investigations have shown that the stability of the nitro compounds is increased by the dioxolane group. To increase the stability further, a second aromatic ring is inserted via these positions. 5-Nitroindole (Figure 3.14, m/z = 162) is used as a model system to analyze the stability of such systems.

UV spectra in aqueous solution show, that the UV absorption of the aromatic π-system is blue shifted compared to indole. Based on the absorption region of indole in a molecular beam [170, 171] at 283 nm, R2PI spectra have been recorded for 5-nitroindole. No parent ion has been obtained; the mass spectra recorded via five different wavelengths are depicted in Figure 3.28. In agreement to the results for the other nitro aromatic compounds, the fragments of 132 Da and 116 Da result from the loss of NO and NO_2. However, the fragment of 93 Da can only be explained by a more complex reaction, e.g. the loss of the nitrogen containing five-membered ring as well as releasing NO under formation of a phenoxy radical.

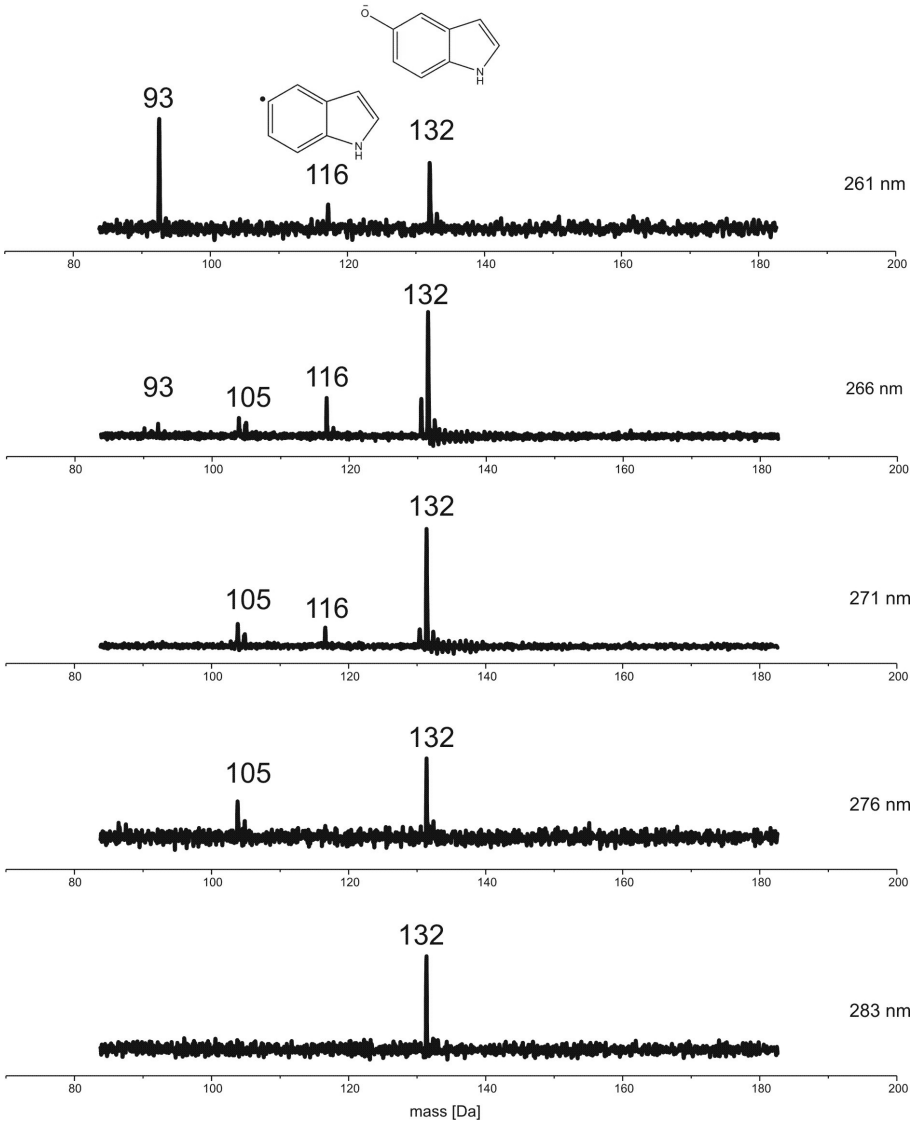

Figure 3.28: Fragmentation pattern of 5-nitroindole at different excitation energies. Most prominent fragments occur at 93 Da, 116 Da and 132 Da.

The one-color R2PI spectrum via the mass trace of the fragment of 132 Da (loss of NO) in the range of 35840 - 38150 cm^{-1} is depicted in Figure 3.29. It exhibits a broad absorption with two maxima at 36791 cm^{-1} and 36941 cm^{-1}. The attempt to apply two-color R2PI spectroscopy in order to reduce the excess energy in the ion and thus prevent fragmentation did not yield a parent ion, due to the fact that fragmentation occurs in the excited state after electronic excitation.

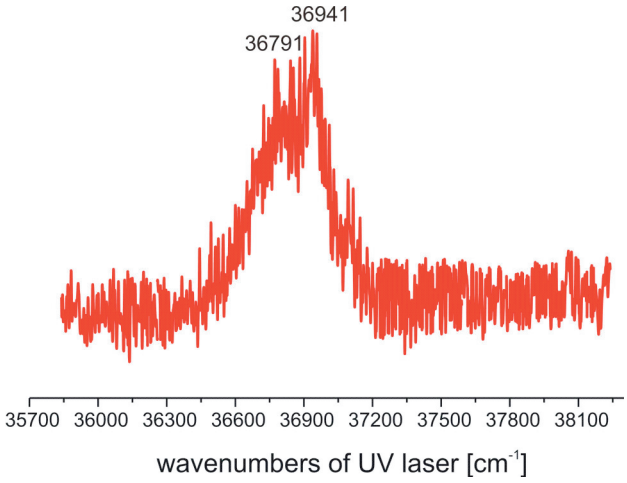

Figure 3.29: R2PI spectrum recorded via the mass trace of the fragment of 132 Da.

3.5.6 Summary

It is known, that caged compounds based on nitro aromatics are very reactive in the excited state. For analyzing these species by combined IR/UV spectroscopy, a parent ion is desirable. Thus the caged compounds have to be stabilized. The investigations focused on caged compounds based on *o*-nitrobenzene which react intramolecularly after electronic excitation. Analyses in molecular beam experiments provide no evidence for the proposed reaction mechanism, instead fragmentation occurred and no parent ion has been obtained. The loss of NO has been observed for all substances which implies a rearrangement in the excited state. It is shown, that the stability of the nitro aromatic compounds depends strongly on the substituent in *m*- and *p*-position, e.g. the species with a dioxolane group exhibit the parent ion as predominant signal (for the molecule without a side chain in *o*-position). The occurrence of the predominant signal highly depends on the excitation

wavelength: In the case of the shorter wavelength of 230 nm (excitation in the range of transition (I)) fragments of higher masses are preferred.

The wavelength depending mass spectrometry in combination with one-color or two-color R2PI spectroscopy as well as IR/R2PI spectroscopy on the resulting fragments yield information on reaction channels and mechanisms as well as a characterization of reaction products. In order to obtain more detailed insights into structural changes and reactions in complete molecules, it is necessary to choose less reactive but selective species based on e.g. coumarins.

4. Summary and Outlook

This thesis is focused on the analysis of primary steps of elementary photoinduced reactions. Especially excited state proton transfer reactions have been investigated with combined IR/UV spectroscopy: The IR spectra of the electronic ground states as well as of the electronically excited states of 3-hydroxyflavone (3-HF), 2-(2-naphthyl)-3-hydroxychromone (2-NHC) and 2,5-dihydroxybenzoic acid (DHB) have been recorded in a supersonic jet.

In the case of DHB the OH stretching vibrations as well as the C=O stretching vibration which are directly involved in the proton transfer have been analyzed in the electronic ground state, the electronically excited state and - for the first time in the mid IR region - in the ionic state. Whereas the hydrogen bonded OH stretching vibration is strongly red shifted and broadened, the C=O stretching vibration is observed in all states, yielding information on the proton transfer reaction. To record the IR spectrum in the range of the C=O stretching vibrations in the electronically excited state, UV+(IR+UV) spectroscopy is applied for the first time. It is an alternative method to the IR/R2PI technique for electronically excited states (UV/IR/UV). Based on the IR spectra for the electronically excited state, a hydrogen dislocation is observed for DHB instead of a proton or hydrogen transfer.

3-HF and 2-NHC are the second molecules investigated with respect to a proton transfer reaction, which was already confirmed via fluorescence spectroscopy in both cases[105, 131]. IR/R2PI (UV/IR/UV) spectroscopy has been introduced subsequent to a reaction in the excited state, yielding direct structural information on the reaction product: The IR spectra of the tautomeric forms have been recorded successfully subsequent to an excited state proton transfer and can unambiguously be assigned by comparing the spectrum to TDDFT calculations. Thus direct structural information about the proton transferred structure has been obtained.

Furthermore the aggregates of 3-HF with water molecules were investigated with respect to proton wire reactions. Other model systems for proton wires such as the aggregates of 7-hydroxyquinolin[21-35] and 7-azaindole[36-40] with different solvent molecules were investigated by fluorescence, UV and combined UV/UV spectroscopy. Furthermore the excited state proton transfer of 3-HF$(H_2O)_2$ was discussed controversially

in literature[113, 123, 124, 133]; however, all investigations focused on fluorescence spectroscopy. Thus for both, 7-hydroxyquinolin and 7-azaindole as well as for 3-HF$(H_2O)_2$ no direct structural assignments for the excited states were obtained. In contrast to these analyses, combined UV/IR/UV spectroscopy of the electronically excited state of 3-HF$(H_2O)_2$ yields direct structural information on the product of the proton transfer. Two isomers are assigned to the electronic ground state by comparing the IR spectrum to DFT calculations, either one (*D* structure) or both water molecules (*I* structure) are inserted into the hydrogen bond of 3-HF. In the electronically excited state, the *D* isomer can unambiguously be assigned by comparing the experimentally obtained frequencies to TDDFT calculations, but an overlay of both structures is probable. No proton transfer leading to the tautomeric forms occurs, which is due to an energy barrier between the two geometries. By increasing the energy of the excitation laser, the proton transfer of the *D* structure is induced and analyzed by IR spectroscopy: The experimentally obtained frequencies fit only to the tautomeric form of the *D* structure. Thus after vertical excitation the normal form of the dihydrate is assigned, but by increasing the excitation energy, a proton transfer along a water molecule is induced leading to the tautomeric form. Therefore the dihydrate of 3-HF represents the first isolated proton wire investigated by combined IR/UV spectroscopy in the excited state, yielding unambiguous structural information.

Photoinduced reactions involve not only singlet but also triplet states. Thus xanthone is chosen as a model system to analyze excited triplet states due to its efficient *ISC* after excitation to the S_2 state. UV/IR/UV spectroscopy has been applied for the first time to triplet states of isolated molecules in a molecular beam experiment: The IR spectrum of the T_1 state has been recorded successfully after the *ISC* into the triplet manifold without using any messenger molecules, and the obtained frequencies can be assigned by comparing the spectrum to DFT calculations. Thus IR/R2PI spectroscopy offers the possibility to investigate not only excited singlet states involved in photoinduced reactions, but also triplet states of isolated reactive molecules.

Caged Compounds release active components in the excited state. The proposed reaction scheme cannot be observed due to fragmentation after photoexcitation. Still rearrangements in the excited states are observed and analyzed via the fragmentation pathways.

Due to the fact that the electronic transitions of the two isomers of 3-HF$(H_2O)_2$ are overlaid, the IR spectrum of the electronic ground state (as well as the IR spectrum of the electronically excited state) is contributable to two isomers. To verify the assignment of the obtained vibrational transitions to the corresponding geometries, IR/IR/UV hole burning spectroscopy[85] (cf. Chapter 2.2.3) will be applied to the S_0 state in future work. Furthermore the question whether the IR spectrum of the excited state of the 3-HF$(H_2O)_2$ cluster is due to only one structure or an overlay of two isomers will be clarified by applying the IR/UV/IR/UV technique, another variant of combined IR/UV spectroscopy: The first IR photon arrives prior to the first UV photon. It is fixed to a vibrational transition of the electronic ground state, depopulating the vibrational ground state of the corresponding isomer. Thus less molecules of this geometry are excited to the S_1 state by the first UV photon. The second IR photon arrives between the first and the second UV photon. An IR spectrum of the excited state is obtained by scanning the second IR laser. If vibrational transitions belong to the same isomer whose vibrational ground state is depopulated by the first IR photon in the electronic ground state, these are considerably smaller than the other bands of the spectrum. By applying this technique to the dihydrate of 3-HF, the question whether two isomers contribute to the IR spectrum of the S_1 state will be clarified. Furthermore the assignment of the vibrational transitions can be confirmed by discriminating the two isomers with this technique.

5. Zusammenfassung und Ausblick

Der Schwerpunkt dieser Arbeit liegt auf der Analyse von Primärschritten photoinduzierter Elementarreaktionen. Insbesondere Protonentransferreaktionen in elektronisch angeregten Zuständen wurden mit kombinierter IR/UV-Spektroskopie untersucht: IR-Spektren der elektronischen Grundzustände sowie der elektronisch angeregten Zustände von 3-Hydroxyflavon (3-HF), 2-(2-Naphthyl)-3-hydroxychromon (2-NHC) und 2,5-Dihydroxybenzoesäure (DHB) wurden in einem Molekularstrahl aufgenommen.

Im Fall des DHBs wurden die OH Streckschwingungen sowie die C=O Streckschwingungen die direkt am Protonentransfer beteiligt sind im elektronischen Grund-, im elektronisch angeregten und - zum ersten Mal im mittleren IR-Bereich - im ionischen Zustand analysiert. Während die wasserstoffbrückengebundene OH-Streckschwingung stark rotverschoben und verbreitert ist, wurde die C=O Streckschwingung in allen Zuständen gemessen und so Informationen über den Protonentransfer gewonnen. Um das IR-Spektrum des elektronisch angeregten Zustands im Bereich der C=O Streckschwingungen aufzunehmen, wurde die UV+(IR+UV)-Spektroskopie zum ersten Mal angewendet. Dies ist eine Alternative zur IR/R2PI-Technik (UV/IR/UV) für elektronisch angeregt Zustände. Basierend auf den IR-Spektren des angeregten Zustands konnte eine Wasserstoffdelokalisierung an Stelle eines Protonen- oder Wasserstofftransfers zugeordnet werden.

Des Weiteren wurden 3-HF und 2-NHC im Hinblick auf einen Protonentransfer im elektronisch angeregten Zustand untersucht. Dieser wurde in beiden Fällen bereits durch Fluoreszenzspektroskopie bestätigt[105, 131]. IR/R2PI-Spektroskopie (UV/IR/UV) zur Untersuchung elektronisch angeregter Zustände im Anschluss an einen Protonentransfer wurde eingeführt, so dass direkte strukturelle Informationen über das Reaktionsprodukt erhalten wurden: Das IR-Spektrum der tautomeren Form wurde erfolgreich nach einem Protonentransfer im elektronisch angeregten Zustand aufgenommen und kann durch einen Vergleich mit TDDFT-Rechnungen eindeutig zugeordnet werden. Folglich wurden direkte strukturelle Informationen über die protonentransferierte Struktur erhalten.

Darüber hinaus wurden Aggregate von 3-HF mit Wassermolekülen im Hinblick auf Protonenleiterreaktionen untersucht. Weitere Modellsysteme für Protonenleiter wie zum

Beispiel 7-Hydroxychinolin[21-35] und 7-Azaindol[36-40] mit verschiedenen Solvensmolekülen wurden bereits mit Fluoreszenz-, UV- und kombinierter UV/UV-Spektroskopie untersucht. Des Weiteren wird der Protonentransfer des 3-HF$(H_2O)_2$ in der Literatur kontrovers diskutiert[113, 123, 124, 133], allerdings wurde bislang nur Fluoreszenzspektroskopie für die Analyse angewendet. Demnach wurden sowohl für 7-Hydroxychinolin und 7-Azaindol als auch für das 3-HF$(H_2O)_2$ keine direkten Strukturzuordnungen für den angeregten Zustand erhalten. Im Gegensatz zu diesen Analysen liefert kombinierte UV/IR/UV-Spektroskopie direkte strukturelle Informationen über das Produkt des Protonentransfers. Zwei Isomere werden dem elektronischen Grundzustand durch Vergleich des IR-Spektrums mit DFT-Rechnungen zugeordnet: Entweder ist eins (*D* Struktur) oder beide Wassermoleküle (*I* Struktur) in die Wasserstoffbrücke von 3-HF insertiert. Im elektronisch angeregten Zustand kann Isomer *D* durch Vergleich der experimentell erhaltenen Banden mit TDDFT-Rechnungen eindeutig zugeordnet werden, allerdings ist eine Überlagerung der beiden Geometrien wahrscheinlich. Es wurde kein Protonentransfer beobachtet, der zur tautomeren Form der *D* oder *I* Struktur führt. Dies liegt an einer Energiebarriere zwischen den beiden Geometrien. Durch eine Erhöhung der Energie des Anregungslasers wird der Protonentransfer im *D* Isomer induziert und mit IR-Spektroskopie analysiert. Die erhaltenen Frequenzen können eindeutig der tautomeren Form der *D* Struktur zugeordnet werden. Demnach wird nach vertikaler Anregung die normale Form des Dihydrates zugeordnet, während durch eine Erhöhung der Anregungsenergie ein Protonentransfer entlang eines Wassermoleküls induziert wird, der zur tautomeren Form führt. Folglich repräsentiert 3-HF$(H_2O)_2$ den ersten isolierten Protonenleiter, für den eindeutige strukturelle Informationen mit kombinierter IR/UV-Spektroskopie im elektronisch angeregten Zustand erhalten wurden.

Da neben elektronisch angeregten Singulett-Zuständen auch Triplett-Zustände an photoinduzierten Reaktionen beteiligt sind, wurde Xanthon mit einem effizienten *ISC* nach Anregung in den S_2-Zustand als Modellsystem gewählt, um Triplett-Zustände zu analysieren. UV/IR/UV-Spektroskopie wurde zum ersten Mal auf Triplett-Zustände im Molekularstrahl angewendet: Das IR-Spektrum des T_1-Zustands wurde erfolgreich nach einem *ISC* in die Triplettmannigfaltigkeit ohne die Benutzung von “messenger” Molekülen aufgenommen, und die experimentell erhaltenen Frequenzen können durch einen Vergleich mit DFT-Rechnungen zugeordnet werden. Demnach bietet IR/R2PI-

Spektroskopie (UV/IR/UV) die Möglichkeit sowohl angeregte Singulett- als auch Triplett-Zustände isolierter reaktiver Moleküle zu analysieren.

Caged Compounds werden eingesetzt um nach Photoanregung Wirkstoffe freizusetzen. Das vorgeschlagene Reaktionsschema konnte nicht beobachtet werden, da die Moleküle nach Photoanregung stark fragmentieren. Trotzdem konnte durch eine Analyse der beobachteten Fragmente eine Umlagerung im elektronisch angeregten Zustand nachgewiesen werden.

Da die elektronischen Übergänge der beiden Isomere des 3-HF$(H_2O)_2$ überlagern, ist das IR-Spektrum des S_0-Zustands (sowie das des elektronisch angeregten Zustands) einer Überlagerung der beiden Strukturen zugeordnet worden. Um die Zuordnung der Banden zu den entsprechenden Isomeren zu bestätigen, wird in Zukunft die IR/IR/UV-Lochbrenn-Spektroskopie[85] (s. Kapitel 2.2.3) auf den elektronischen Grundzustand angewendet. Des Weiteren wird die Frage ob das IR-Spektrum des angeregten Zustands von 3-HF$(H_2O)_2$ durch eine Überlagerung der beiden Isomere entsteht durch Anwendung der IR/UV/IR/UV-Technik - einer weiteren Variante kombinierter IR/UV-Spektroskopie - geklärt: Das erste IR-Photon wird vor dem ersten UV-Photon eingestrahlt und auf eine Schwingungsbande des S_0-Zustands gestellt. Dadurch wird der Schwingungs-grundzustand des entsprechenden Isomers depopuliert und weniger Moleküle dieser Struktur werden durch das erste UV-Photon in den S_1-Zustand angeregt. Das zweite IR-Photon wird zwischen dem ersten und dem zweiten UV-Photon eingestrahlt. Durch das Durchstimmen des zweiten IR-Lasers wird ein Spektrum des elektronisch angeregten Zustands erhalten. Falls Schwingungsübergänge zu demselben Isomer gehören, dessen Schwingungsgrundzustand von dem ersten IR-Photon im S_0-Zustand depopuliert wurde, sind diese deutlich kleiner als die anderen Banden des Spektrums. Durch Anwendung dieser Technik auf das Dihydrat von 3-HF wird die Frage geklärt ob das IR-Spektrum des S_1-Zustands auf zwei Isomere zurückzuführen ist. Des Weiteren kann die Zuordnung der Schwingungsbanden zu der jeweiligen Struktur bestätigt werden.

6. References

[1] A. L. Sobolewski, W. Domcke, *Chemical Physics* **2003**, *294*, 73.
[2] C. Plutzer, I. Hunig, K. Kleinermanns, *Physical Chemistry Chemical Physics* **2003**, *5*, 1158.
[3] I. Hunig, C. Plutzer, K. A. Seefeld, D. Lowenich, M. Nispel, K. Kleinermanns, *Chemphyschem* **2004**, *5*, 1427.
[4] T. Schultz, E. Samoylova, W. Radloff, I. V. Hertel, A. L. Sobolewski, W. Domcke, *Science* **2004**, *306*, 1765.
[5] A. L. Sobolewski, W. Domcke, *Physical Chemistry Chemical Physics* **2004**, *6*, 2763.
[6] K. Strupat, M. Karas, F. Hillenkamp, *International Journal of Mass Spectrometry and Ion Processes* **1991**, *111*, 89.
[7] M. Karas, F. Hillenkamp, *Analytical Chemistry* **1988**, *60*, 2299.
[8] J. F. Nagle, H. J. Morowitz, *Proceedings of the National Academy of Sciences of the United States of America* **1978**, *75*, 298.
[9] J. F. Nagle, S. Tristramnagle, *Journal of Membrane Biology* **1983**, *74*, 1.
[10] E. PebayPeyroula, G. Rummel, J. P. Rosenbusch, E. M. Landau, *Science* **1997**, *277*, 1676.
[11] H. Luecke, H. T. Richter, J. K. Lanyi, *Science* **1998**, *280*, 1934.
[12] H. Luecke, B. Schobert, H. T. Richter, J. P. Cartailler, J. K. Lanyi, *Science* **1999**, *286*, 255.
[13] L. Baciou, H. Michel, *Biochemistry* **1995**, *34*, 7967.
[14] A. Remy, K. Gerwert, *Nature Structural Biology* **2003**, *10*, 637.
[15] J. Tandori, P. Sebban, H. Michel, L. Baciou, *Biochemistry* **1999**, *38*, 13179.
[16] R. Pomes, B. Roux, *Biophysical Journal* **2002**, *82*, 2304.
[17] R. Pomes, C. H. Yu, *Frontiers in Bioscience* **2003**, *8*, D1288.
[18] B. Roux, *Accounts of Chemical Research* **2002**, *35*, 366.
[19] N. Agmon, *Chemical Physics Letters* **1995**, *244*, 456.
[20] D. Marx, M. E. Tuckerman, J. Hutter, M. Parrinello, *Nature* **1999**, *397*, 601.
[21] Y. Matsumoto, T. Ebata, N. Mikami, *Journal of Physical Chemistry A* **2002**, *106*, 5591.
[22] A. Bach, S. Leutwyler, *Journal of Chemical Physics* **2000**, *112*, 560.
[23] A. Bach, S. Coussan, A. Muller, S. Leutwyler, *Journal of Chemical Physics* **2000**, *113*, 9032.
[24] S. Coussan, A. Bach, S. Leutwyler, *Journal of Physical Chemistry A* **2000**, *104*, 9864.
[25] A. Bach, S. Coussan, A. Muller, S. Leutwyler, *Journal of Chemical Physics* **2000**, *112*, 1192.
[26] S. Coussan, M. Meuwly, S. Leutwyler, *Journal of Chemical Physics* **2001**, *114*, 3524.
[27] S. Coussan, C. Manca, C. Tanner, A. Bach, S. Leutwyler, *Journal of Chemical Physics* **2003**, *119*, 3774.
[28] A. Bach, C. Tanner, C. Manca, H. M. Frey, S. Leutwyler, *Journal of Chemical Physics* **2003**, *119*, 5933.
[29] C. Tanner, C. Manca, S. Leutwyler, *Science* **2003**, *302*, 1736.
[30] C. Tanner, C. Manca, S. Leutwyler, *Chimia* **2004**, *58*, 234.
[31] C. Manca, C. Tanner, S. Leutwyler, *Chimia* **2004**, *58*, 287.

[32] C. Manca, C. Tanner, S. Leutwyler, *International Reviews in Physical Chemistry* **2005**, *24*, 457.
[33] C. Manca, C. Tanner, S. Coussan, A. Bach, S. Leutwyler, *Journal of Chemical Physics* **2004**, *121*, 2578.
[34] C. Tanner, C. Manca, S. Leutwyler, *Journal of Chemical Physics* **2005**, *122*, 11.
[35] C. Tanner, M. Thut, A. Steinlin, C. Manca, S. Leutwyler, *Journal of Physical Chemistry A* **2006**, *110*, 1758.
[36] K. Sakota, Y. Kageura, H. Sekiya, *Journal of Chemical Physics* **2008**, *129*, 10.
[37] K. Sakota, Y. Komoto, M. Nakagaki, W. Ishikawa, H. Sekiya, *Chemical Physics Letters* **2007**, *435*, 1.
[38] K. Sakota, N. Inoue, Y. Komoto, H. Sekiya, *Journal of Physical Chemistry A* **2007**, *111*, 4596.
[39] A. Hara, K. Sakota, M. Nakagaki, H. Sekiya, *Chemical Physics Letters* **2005**, *407*, 30.
[40] T. B. C. Vu, I. Kalkman, W. L. Meerts, Y. N. Svartsov, C. Jacoby, M. Schmitt, *Journal of Chemical Physics* **2008**, *128*, 8.
[41] J. H. Kaplan, B. Forbush, J. F. Hoffman, *Biochemistry* **1978**, *17*, 1929.
[42] J. Engels, E. J. Schlaeger, *Journal of Medicinal Chemistry* **1977**, *20*, 907.
[43] J. Engels, R. Reidys, *Experientia* **1978**, *34*, 14.
[44] N. J. Turro, *Modern Molecular Chemistry, The Benjamin/Cummings Publishing Company, Menlo Park* **1978**.
[45] C. M. Marian, F. Schneider, M. Kleinschmidt, J. Tatchen, *European Physical Journal D* **2002**, *20*, 357.
[46] P. S. Drzaic, J. I. Brauman, *Journal of the American Chemical Society* **1984**, *106*, 3443.
[47] R. Weinkauf, P. Schanen, A. Metsala, E. W. Schlag, M. Burgle, H. Kessler, *Journal of Physical Chemistry* **1996**, *100*, 18567.
[48] J. Schiedt, R. Weinkauf, *Chemical Physics Letters* **1997**, *266*, 201.
[49] P. G. Wenthold, J. B. Kim, W. C. Lineberger, *Journal of the American Chemical Society* **1997**, *119*, 1354.
[50] S. Rentsch, J. P. Yang, W. Paa, E. Birckner, J. Schiedt, R. Weinkauf, *Physical Chemistry Chemical Physics* **1999**, *1*, 1707.
[51] T. R. Taylor, R. T. Bise, K. R. Asmis, D. M. Neumark, *Chemical Physics Letters* **1999**, *301*, 413.
[52] K. Remmers, R. G. Satink, G. von Helden, H. Piest, G. Meijer, W. L. Meerts, *Chemical Physics Letters* **2000**, *317*, 197.
[53] R. H. Page, Y. R. Shen, Y. T. Lee, *Journal of Chemical Physics* **1988**, *88*, 4621.
[54] C. Riehn, C. Lahmann, B. Wassermann, B. Brutschy, *Chemical Physics Letters* **1992**, *197*, 443.
[55] S. Tanabe, T. Ebata, M. Fujii, N. Mikami, *Chemical Physics Letters* **1993**, *215*, 347.
[56] T. S. Zwier, *Annual Review of Physical Chemistry* **1996**, *47*, 205.
[57] M. Gerhards, C. Unterberg, A. Gerlach, *Physical Chemistry Chemical Physics* **2002**, *4*, 5563.
[58] F. Huisken, A. Kulcke, D. Voelkel, C. Laush, J. M. Lisy, *Applied Physics Letters* **1993**, *62*, 805.
[59] D. S. Bethune, A. C. Luntz, *Applied Physics B-Photophysics and Laser Chemistry* **1986**, *40*, 107.
[60] M. Gerhards, *Optics Communications* **2004**, *241*, 493.

[61] D. Oepts, A. F. G. Vandermeer, P. W. Vanamersfoort, in *6th International Conference on Infrared Physics (CIRP 6) - Topical Conference on Infrared Lasers*, Pergamon-Elsevier Science Ltd, Ascona, Switzerland, **1994**, pp. 297.
[62] J. M. Bakker, L. M. Aleese, G. Meijer, G. von Helden, *Physical Review Letters* **2003**, *91*, 4.
[63] P. Carcabal, R. T. Kroemer, L. C. Snoek, J. P. Simons, J. M. Bakker, I. Compagnon, G. Meijer, G. von Helden, *Physical Chemistry Chemical Physics* **2004**, *6*, 4546.
[64] P. M. Johnson, *Journal of Chemical Physics* **1976**, *64*, 4143.
[65] V. S. Antonov, I. N. Knyazev, V. S. Letokhov, *Optics Letters* **1978**, *3*, 37.
[66] U. Boesl, H. J. Neusser, E. W. Schlag, *Zeitschrift Fur Naturforschung Section a-a Journal of Physical Sciences* **1978**, *33*, 1546.
[67] R. J. Lipert, S. D. Colson, *Journal of Physical Chemistry* **1989**, *93*, 3894.
[68] Y. Chen, M. R. Topp, *Chemical Physics* **2002**, *283*, 249.
[69] Y. Chen, P. M. Palmer, M. R. Topp, *International Journal of Mass Spectrometrie* **2002**, *220*, 231.
[70] T. H. Walther, H. Bitto, T. K. Minton, J. R. Huber, *Chemical Physics Letters* **1994**, *231*, 64.
[71] T. Ebata, N. Mizouchi, T. Watanabe, N. Mikami, *Journal of Physical Chemistry* **1996**, *100*, 546.
[72] M. Gerhards, M. Schiwek, C. Unterberg, K. Kleinermanns, *Chemical Physics Letters* **1998**, *297*, 522.
[73] A. Funk, *current dissertation, Kaiserslautern*.
[74] L. C. Zhu, P. Johnson, *Journal of Chemical Physics* **1991**, *94*, 5769.
[75] W. C. Wiley, I. H. McLaren, *Review of Scientific Instruments* **1955**, *26*, 1150.
[76] G. Reiser, W. Habenicht, K. Mullerdethlefs, *Chemical Physics Letters* **1988**, *152*, 119.
[77] K. Mullerdethlefs, E. W. Schlag, *Annual Review of Physical Chemistry* **1991**, *42*, 109.
[78] K. Müller-Dethlefs, *High Resolution Laser Photoionization and Photolectrons Studies, Hrsgb. I. Powis, T. Baer, C. Y. Ng, J. Wiley&Sons Ltd, New York* **1995**.
[79] K. Muller-Dethlefs, E. W. Schlag, *Angewandte Chemie-International Edition* **1998**, *37*, 1346.
[80] H. J. Dietrich, R. Lindner, K. Mullerdethlefs, *Journal of Chemical Physics* **1994**, *101*, 3399.
[81] W. A. Chupka, *Journal of Chemical Physics* **1993**, *99*, 5800.
[82] W. A. Chupka, *Journal of Chemical Physics* **1993**, *98*, 4520.
[83] A. Mitsuzuka, A. Fujii, T. Ebata, N. Mikami, *Journal of Chemical Physics* **1996**, *105*, 2618.
[84] R. K. Frost, F. C. Hagemeister, C. A. Arrington, D. Schleppenbach, T. S. Zwier, *Journal of Chemical Physics* **1996**, *105*, 2605.
[85] V. A. Shubert, T. S. Zwier, *Journal of Physical Chemistry A* **2007**, *111*.
[86] A. Weller, *Naturwissenschaften* **1955**, *42*, 175.
[87] A. Weller, *Zeitschrift Fur Elektrochemie* **1956**, *60*, 1144.
[88] A. Weller, *Progress in Reaction Kinetics and Mechanism* **1961**, *1*, 187.
[89] P. B. Bisht, H. Petek, K. Yoshihara, U. Nagashima, *Journal of Chemical Physics* **1995**, *103*, 5290.
[90] T. Yahagi, A. Fujii, T. Ebata, N. Mikami, *Journal of Physical Chemistry A* **2001**, *105*, 10673.

[91] A. Abou El-Nasr, A. Fujii, T. Ebata, N. Mikami, *Molecular Physics* **2005**, *103*, 1561.
[92] A. L. Sobolewski, W. Domcke, *Chemical Physics* **1998**, *232*, 257.
[93] A. L. Sobolewski, W. Domcke, *Physical Chemistry Chemical Physics* **1999**, *1*, 3065.
[94] A. L. Sobolewski, W. Domcke, *Journal of Physical Chemistry A* **2004**, *108*, 10917.
[95] A. J. A. Aquino, H. Lischka, C. Hattig, *Journal of Physical Chemistry A* **2005**, *109*, 3201.
[96] A. L. Sobolewski, W. Domcke, *Physical Chemistry Chemical Physics* **2006**, *8*, 3410.
[97] S. Jang, S. Il Jin, C. R. Park, *Bulletin of the Korean Chemical Society* **2007**, *28*, 2343.
[98] A. A. Abou El-Nasr, A. Fujii, T. Ebata, N. Mikami, *Chemical Physics Letters* **2003**, *376*, 788.
[99] C. A. Southern, D. H. Levy, G. M. Florio, A. Longarte, T. S. Zwier, *Journal of Physical Chemistry A* **2003**, *107*, 4032.
[100] C. A. Southern, D. H. Levy, J. A. Stearns, G. M. Florio, A. Longarte, T. S. Zwier, *Journal of Physical Chemistry A* **2004**, *108*, 4599.
[101] J. A. Stearns, A. Das, T. S. Zwier, *Physical Chemistry Chemical Physics* **2004**, *6*, 2605.
[102] V. Karbach, R. Knochenmuss, *Rapid Communications in Mass Spectrometry* **1998**, *12*, 968.
[103] Q. Lin, R. Knochenmuss, *Rapid Communications in Mass Spectrometry* **2001**, *15*, 1422.
[104] J. B. Harborne, C. A. Williams, *Phytochemistry* **2000**, *55*, 481.
[105] P. K. Sengupta, M. Kasha, *Chemical Physics Letters* **1979**, *68*, 382.
[106] G. J. Woolfe, P. J. Thistlethwaite, *Journal of the American Chemical Society* **1981**, *103*, 6916.
[107] M. Itoh, K. Tokumura, Y. Tanimoto, Y. Okada, H. Takeuchi, I. Obi, I. Tanaka, *Journal of the American Chemical Society* **1982**, *104*, 4146.
[108] A. J. G. Strandjord, S. H. Courtney, D. M. Friedrich, P. F. Barbara, *Journal of Physical Chemistry* **1983**, *87*, 1125.
[109] D. McMorrow, T. P. Dzugan, T. J. Aartsma, *Chemical Physics Letters* **1984**, *103*, 492.
[110] M. Itoh, Y. Fujiwara, M. Sumitani, K. Yoshihara, *Journal of Physical Chemistry* **1986**, *90*, 5672.
[111] B. Dick, N. P. Ernsting, *Journal of Physical Chemistry* **1987**, *91*, 4261.
[112] G. A. Brucker, D. F. Kelley, *Journal of Physical Chemistry* **1987**, *91*, 2856.
[113] G. A. Brucker, D. F. Kelley, *Journal of Physical Chemistry* **1988**, *92*, 3805.
[114] G. A. Brucker, T. C. Swinney, D. F. Kelley, *Journal of Physical Chemistry* **1991**, *95*, 3190.
[115] T. C. Swinney, D. F. Kelley, *Journal of Physical Chemistry* **1991**, *95*, 10369.
[116] B. J. Schwartz, L. A. Peteanu, C. B. Harris, *Journal of Physical Chemistry* **1992**, *96*, 3591.
[117] S. M. Ormson, D. LeGourrierec, R. G. Brown, P. Foggi, *Journal of the Chemical Society-Chemical Communications* **1995**.
[118] S. Ameer-Beg, S. M. Ormson, R. G. Brown, P. Matousek, M. Towrie, E. T. J. Nibbering, P. Foggi, F. V. R. Neuwahl, *Journal of Physical Chemistry A* **2001**, *105*, 3709.

[119] A. N. Bader, F. Ariese, C. Gooijer, *Journal of Physical Chemistry A* **2002**, *106*, 2844.
[120] A. N. Bader, V. G. Pivovarenko, A. P. Demchenko, F. Ariese, C. Gooijer, *Journal of Physical Chemistry B* **2004**, *108*, 10589.
[121] N. P. Ernsting, B. Dick, *Chemical Physics* **1989**, 181.
[122] M. Itoh, H. Kurokawa, *Chemical Physics Letters* **1982**, *91*, 487.
[123] A. Ito, Y. Fujiwara, M. Itoh, *Journal of Chemical Physics* **1992**, *96*, 7474.
[124] M. Itoh, *Pure & Applied Chemistry* **1993**, *65*, 1629.
[125] A. Mühlpfordt, T. Bultmann, N. P. Ernsting, *Chemical Physics* **1994**, *181*, 447.
[126] J. H. Looker, W. W. Hanneman, *Journal of Organic Chemistry* **1962**, *27*, 381.
[127] B. L. Shaw, T. H. Simpson, *Chelate Systems* **1955**, 655.
[128] J. M. Petrosky, C. D. S. Valente, E. P. Kelson, S. Collins, *Journal of Physical Chemistry A* **2002**, *106*, 11714.
[129] A. Vavra, R. Linder, K. Kleinermanns, *Chemical Physics Letters* **2008**, *463*, 349.
[130] *NIST Chemistry WebBook*.
[131] M. Itoh, Y. Fujiwara, M. Matsudo, A. Higashikata, K. Tokumura, *Journal of Physical Chemistry* **1990**, *94*, 8146.
[132] H. Mukaihata, T. Ohkubo, Y. Fujiwara, M. Itoh, *Chemical Physics Letters* **1993**, *211*, 140.
[133] R. Lehnig, *Dissertation, Regensburg 2004*.
[134] R. Takasu, Y. Fujiwara, M. Itoh, *Chemical Physics Letters* **1994**, *217*, 478.
[135] J. M. Dawes, S. C. Wallace, *Chemical Physics Letters* **1993**, *208*, 335.
[136] B. Heinz, B. Schmidt, C. Root, H. Satzger, F. Milota, B. Fierz, T. Kiefhaber, W. Zinth, P. Gilch, *Physical Chemistry Chemical Physics* **2006**, *8*, 3432.
[137] H. J. Pownall, J. R. Huber, *Journal of the American Chemical Society* **1971**, *93*, 6429.
[138] H. J. Pownall, R. E. Connors, J. R. Huber, *Chemical Physics Letters* **1973**, *22*, 403.
[139] A. Chakrabarti, N. Hirota, *Journal of Physical Chemistry* **1976**, *80*, 2966.
[140] R. E. Connors, P. S. Walsh, *Chemical Physics Letters* **1977**, *52*, 436.
[141] B. I. Greene, R. M. Hochstrasser, R. B. Weisman, *Journal of Chemical Physics* **1979**, *10*, 1247.
[142] J. C. Scaiano, *Journal of the American Chemical Society* **1980**, *102*, 7747.
[143] H. J. Griesser, R. Bramley, *Chemical Physics Letters* **1981**, *83*, 287.
[144] H. J. Griesser, R. Bramley, *Journal of Luminescence* **1981**, *24/25*, 531.
[145] H. J. Griesser, R. Bramley, *Chemical Physics* **1982**, *67*, 373.
[146] K. A. Abdullah, T. J. Kemp, *Journal of Photochemistry* **1986**, *32*, 49.
[147] R. E. Connors, R. J. Sweeney, F. Cerio, *Journal of Physical Chemistry* **1987**, *91*, 819.
[148] M. Koyanagi, T. Terada, K. Nakashima, *Journal of Chemical Physics* **1988**, *89*, 7349.
[149] H. Murai, M. Minami, Y. J. l´Haya, *Journal of Physical Chemistry* **1988**, *92*, 2120.
[150] M. Koyanagi, T. Terada, *Journal of Luminescence* **1991**, *48 & 49*, 391.
[151] J. J. Cavaleri, K. Prater, R. M. Bowman, *Chemical Physics Letters* **1996**, *259*, 495.
[152] H. Satzger, B. Schmidt, C. Root, W. Zinth, B. Fierz, F. Krieger, T. Kiefhaber, P. Gilch, *Journal of Physical Chemistry A* **2004**, *108*, 10072.
[153] M. Baba, T. Kamei, M. Kiritani, S. Yamauchi, N. Hirota, *Chemical Physics Letters* **1991**, *185*, 354.
[154] Y. Ohshima, T. Fujii, T. Fujita, D. Inaba, M. Baba, *Journal of Physical Chemistry A* **2003**, *107*, 8851.
[155] M. A. El-Sayed, *Journal of Chemical Physics* **1963**, *38*, 2834.

[156] S. Ishijima, M. Higashi, H. Yamaguchi, M. Kubota, T. Kobayashi, *Journal of Electron Spectroscopy and Related Phenomena* **1996**, *82*, 71.
[157] W. Nakanishi, S. Hayashi, Y. Kusuyama, T. Negoro, S. Masuda, H. Mutoh, *Journal of Organic Chemistry* **1998**, *63*, 8373.
[158] I. R. Dunkin, J. Gebicki, M. Kiszka, D. Sanin-Leira, *Spectrochimica Acta Part a-Molecular and Biomolecular Spectroscopy* **1997**, *53*, 2553.
[159] I. R. Dunkin, J. Gebicki, M. Kiszka, D. Sanin-Leira, *Journal of the Chemical Society-Perkin Transactions 2* **2001**, 1414.
[160] F. Bley, K. Schaper, H. Gorner, *Photochemistry and Photobiology* **2008**, *84*, 162.
[161] B. Schade, V. Hagen, R. Schmidt, R. Herbrich, E. Krause, T. Eckardt, J. Bendig, *Journal of Organic Chemistry* **1999**, *64*, 9109.
[162] V. Hagen, B. Dekowski, V. Nache, R. Schmidt, D. Geissler, D. Lorenz, J. Eichhorst, S. Keller, H. Kaneko, K. Benndorf, B. Wiesner, *Angewandte Chemie-International Edition* **2005**, *44*, 7887.
[163] R. Schmidt, D. Geissler, V. Hagen, J. Bendig, *Journal of Physical Chemistry A* **2007**, *111*, 5768.
[164] *Private Communication Timo Fleig and Mihajlo Etinsky*
[165] K. W. D. Ledingham, H. S. Kilic, C. Kosmidis, R. M. Deas, A. Marshall, T. McCanny, R. P. Singhal, A. J. Langley, W. Shaikh, *Rapid Communications in Mass Spectrometry* **1995**, *9*, 1522.
[166] A. M. Wodtke, E. J. Hintsa, Y. T. Lee, *Journal of Physical Chemistry* **1986**, *90*, 3549.
[167] K. J. Castle, J. E. Abbott, X. Z. Peng, W. Kong, *Journal of Physical Chemistry A* **2000**, *104*, 10419.
[168] D. B. Galloway, T. Glenewinkelmeyer, J. A. Bartz, L. G. Huey, F. F. Crim, *Journal of Chemical Physics* **1994**, *100*, 1946.
[169] N. Guchhait, T. Ebata, N. Mikami, *Journal of Chemical Physics* **1999**, *111*, 8438.
[170] J. Hager, S. C. Wallace, *Journal of Physical Chemistry* **1983**, *87*, 2121.
[171] R. M. Helm, M. Clara, T. L. Grebner, H. J. Neusser, *Journal of Physical Chemistry A* **1998**, *102*, 3268.

Appendix A

Experimental Parameters

Tab. A: Experimental parameters used for the investigated molecules (Output energies of the IR laser system for the different spectral ranges are described in Chapter 2.3; the voltages connected to the microchannel plate detector were set to -1700 V (VD1), -926.5 V (VD2) and -154.7 V (VD3) for all substances).

	DHB	**3-HF and 3-HF $(H_2O)_n$**	**2-NHC**	**Xan-thone**	**6-Nitro-piperonyl-alcohol**	**6-Nitro-piperonyl-acetate**	**3,4-Methylendi-oxynitro-benzene**	**3,4-Di-methoxy-nitro-benzene**	**5-Nitro-indole**
$T_{Micro\ chamber}$	130 °C	110 °C	150 °C	95 °C	80 - 90 °C	70 – 80 °C	80 - 100 °C	70 - 90 °C	90 °C
Carrier Gas	He	Ne	He	He	He	He	He	He	He
$p_{Carrier\ Gas}$	2,5 bar	2,5 bar	2,5 bar	2,5 bar	2,5 bar	2,5 bar	2,5 bar	2,5 bar	2,5 bar
VX1 / [V]	87	230	230	230	230	230	230	230	230
VA1 / [V]	1168	4130	4130	4130	4130	4130	4130	4130	4130
VA2 / [V]	1025	3518	3518	3518	3518	3518	3518	3518	3518
MATI Voltage	1.6 V	-	-	-	-	-	-	-	-
$\Delta(UV_1\text{-}UV_2)$	10 ns	6 ns	6 ns	150 ns	<1 ns	<1 ns	<1 ns	<1 ns	<1 ns
$\Delta(IR\text{-}UV_1)$	90 ns	90 ns	90 ns	90 ns	90 ns	90 ns	90 ns	90 ns	90 ns
$\Delta(UV_1\text{-}IR)$	7 ns	4 ns	4 ns	20 ns	-	-	-	-	-
Output Energy UV_1	1 mJ	0,6 mJ	0.6 mJ	0.6 mJ	0,6-2 mJ	0,6-2 mJ	0,6-2 mJ	0,6-2 mJ	0,7 mJ
Outpt Energy UV_2	0.5 mJ	0,4 mJ	0,4 mJ	<20 µJ	0,6-2 mJ	0,6-1 mJ	0,6-1 mJ	0,6-1 mJ	0,4 mJ

Appendix B

Pulsed Operated Apparatus

Two Digital Delay/Pulse Generators are used to control the timing of the various laser systems, the oscilloscope and the pulse for the acceleration voltage. The first Digital Delay/Pulse Generator is self-made and triggered by the pulse driver. It offers four circuit points:

1) Provides the voltage (1-2 V) to separate the direct ions from the Rydberg neutrals for MATI and IR/PIRI experiments.
2) TTL Pulse, triggers the second Digital Delay/Pulse Generator (DG 535, Stanford Research) as well as the flash lamps of the Nd:YAG laser (Spectra-Physics Pro-230) used to pump the IR laser system.
3) and 4) 15V Pulses, trigger the flash lamps of the two Nd:YAG lasers used to generate the UV light.

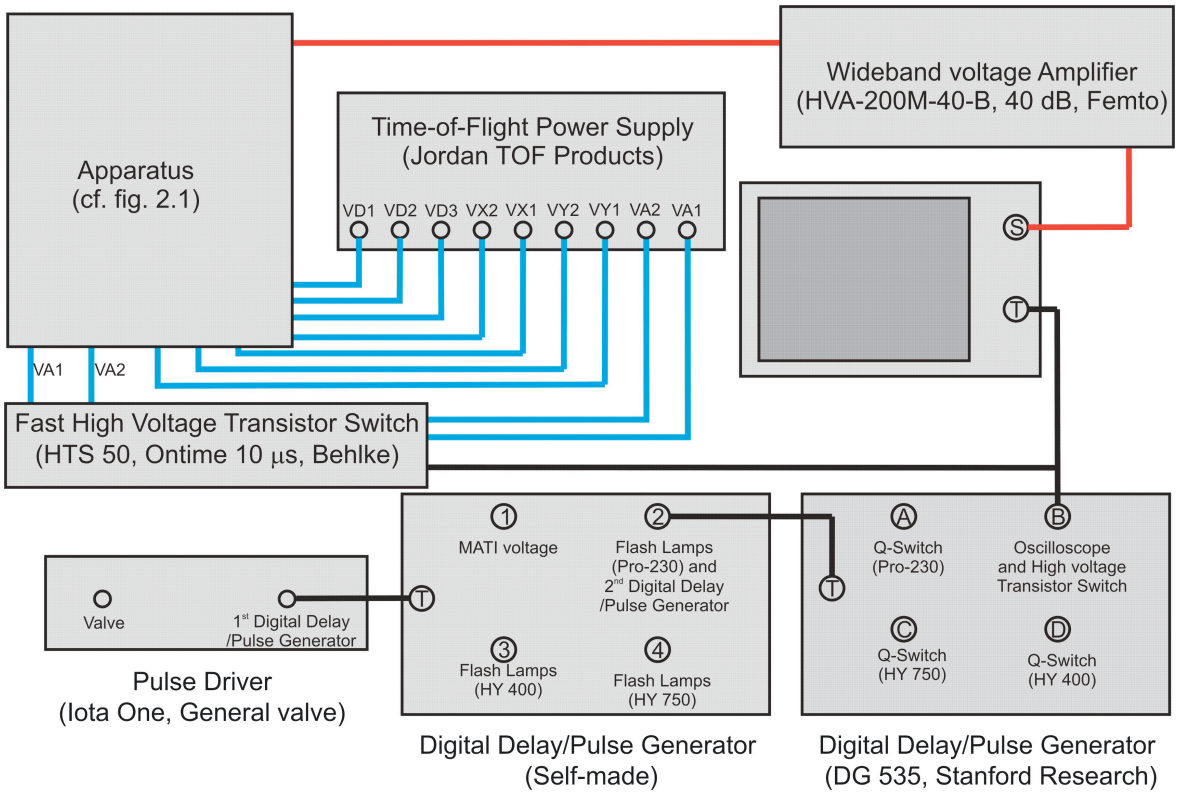

Figure B: Connection scheme for the pulsed operation of the apparatus.

The second Digital Delay/Pulse Generator (DG 535, Stanford Research) offers four circuit points as well, it triggers the applications needing more temporal accuracy (Delay resolution 5 ps):

A) 6.4 V Pulse, triggers the Q-Switch of the Nd:YAG laser pumping the IR system (Spectra-Physics Pro-230).

B) TTL Pulse, triggers the Fast High Voltage Transistor Switch (HTS 50, Ontime 10ms, Behlke) which controls the pulse for the acceleration voltages as well as the oscilloscope (TDS 520, Techtronics).

C) and D) 15 V Pulses, trigger the Q-Switches of the two Nd:YAG lasers pumping the two UV laser systems.

A typical setup for recording IR spectra in the S_1 state of 3-HF and its aggregates with water (carrier gas: Ne) is

1:	769.9 µs	A:	T + 179,8839 µs
2:	589,0 µs	B:	C + 28 µs
3:	540.1 µs	C:	T + 179.9 µs
4:	519.0 µs	D:	C + 32 µs.

The arriving time of the laser beams at the apparatus is changed by adjusting the trigger times for the Q-Switches of the various Nd:YAG lasers. The timing is only shifted on a ns timescale and thus there is no need to adjust the trigger times for the flash lamps. The time delay between flash lamps and Q-Switch is set to

250 µs for Lumonics HY 750
229 µs for Lumonics HY 400 and
180 µs for Spectra-Physics Pro-230.

Appendix C

List of Publications

[I] **Proton/Hydrogen-Transfer Coordinate of 2,5-Dihydroxybenzoic Acid investigated in a Supersonic Beam: Combined IR/UV Spectroscopy in the S_0, S_1 and D_0 States**
H. Fricke, K. Bartl, A. Funk, A. Gerlach, M. Gerhards,
ChemPhysChem **2008**, *9*, 2592

[II] **IR spectroscopy applied subsequent to a proton transfer reaction in the excited state of isolated 3-hydroxyflavone and 2-(2-naphthyl)-3-hydroxychromone**
K. Bartl, A. Funk, K. Schwing, H. Fricke, G. Kock, H.-D. Martin, M. Gerhards,
Physical Chemistry Chemical Physics **2009**, *11*, 1173

[III] **IR/UV spectroscopy on jet cooled 3-hydroxyflavone$(H_2O)_n$ (n=1,2) clusters along proton transfer coordinates in the electronic ground and excited states**
K. Bartl, A. Funk, M. Gerhards,
Journal of Chemical Physics **2008**, *129*, 234306

[IV] **Structure of Isolated Xanthone in the T_1 State Obtained via Combined UV/IR Spectroscopy**
K. Bartl, A. Funk, M. Gerhards,
ChemPhysChem **2009**, *10*, 1882

Eidesstattliche Erklärung

Hiermit bestätige ich, Dipl.-Chem. Kristina Bartl, dass die vorliegende Arbeit gemäß der Promotionsordnung des Fachbereichs Chemie der Technischen Universität Kaiserslautern selbstständig und mit den angegebenen Hilfsmitteln und Quellen angefertigt wurde.

Kaiserslautern, im Juni 2009.